

# On Robust Empirical Likelihood for Nonparametric Regression with Application to Regression Discontinuity Designs

Qin Fang<sup>1</sup>, Shaojun Guo<sup>2</sup>, Yang Hong<sup>3</sup>, and Xinghao Qiao<sup>4</sup>

<sup>1</sup>*University of Sydney Business School, Sydney, Australia*

<sup>2</sup>*Institute of Statistics and Big Data, Renmin University of China, China*

<sup>3</sup>*School of Mathematics, Renmin University of China, China*

<sup>4</sup>*Faculty of Business and Economics, The University of Hong Kong, Hong Kong*

## Abstract

Empirical likelihood serves as a powerful tool for constructing confidence intervals in nonparametric regression and regression discontinuity designs (RDD). The original empirical likelihood framework can be naturally extended to these settings using local linear smoothers, with Wilks' theorem holding only when an undersmoothed bandwidth is selected. However, the generalization of bias-corrected versions of empirical likelihood under more realistic conditions is non-trivial and has remained an open challenge in the literature. This paper provides a satisfactory solution by proposing a novel approach, referred to as robust empirical likelihood, designed for nonparametric regression and RDD. The core idea is to construct robust weights which simultaneously achieve bias correction and account for the additional variability introduced by the estimated bias, thereby enabling valid confidence interval construction without extra estimation steps involved. We demonstrate that the Wilks' phenomenon still holds under weaker conditions in nonparametric regression, sharp and fuzzy RDD settings. Extensive simulation studies confirm the effectiveness of our proposed approach, showing superior performance over existing methods in terms of coverage probabilities and interval lengths. Moreover, the proposed procedure exhibits robustness to bandwidth selection, making it a flexible and reliable tool for empirical analyses. The practical usefulness is further illustrated through applications to two real datasets.

**Keywords:** Empirical likelihood; Local polynomials; Wilks' phenomenon; Regression discontinuity; Robust bias-correction.

# 1 Introduction

Nonparametric regression has emerged as a key tool in statistics and econometrics over recent decades, as it provides a flexible framework for estimation and inference when modeling complex relationships between dependent and independent variables. By avoiding rigid functional form assumptions, this data-driven approach accommodates a wide range of applications, including functional and longitudinal data, time series, regression discontinuity designs (RDD) and many others. RDD, in particular, has gained great attention as a leading quasi-experimental method in causal inference for identifying the effects of treatment assignments on outcomes of interest, and nonparametric local polynomial estimators (Fan and Gijbels; 1996) are now routinely used to estimate the average treatment effect at the cutoff point (Armstrong and Kolesár; 2018; Cattaneo et al.; 2019, 2024). Despite their distinct methodologies and applications, nonparametric regression and RDD exhibit fundamental similarities and share common concerns in constructing confidence intervals. In this paper, we aim to develop an automatic, easy-to-implement yet effective procedure for nonparametric regression and RDD, integrating empirical likelihood (EL) with local polynomial smoothing and bias correction to achieve robust and valid inference without extra estimation steps involved. Our method produces confidence intervals with close-to-correct empirical coverage across a broader range of bandwidth choices and thus provides a satisfactory solution for a long-standing challenge in the EL literature.

Empirical likelihood, originally introduced by Owen (1988, 1990), is a nonparametric likelihood-based inference method that has seen a wave of advancements in its applications to parametric, semiparametric, and nonparametric models; see, e.g., Kitamura et al. (2004); Xue and Zhu (2007b); Chen and Van Keilegom (2009); Bravo et al. (2020); Matsushita and Otsu (2021); Xue (2023), and Yu and Bondell (2024). Its appealing properties include the automatic determination of confidence region shapes, the capacity to incorporate side information through constraints, Bartlett correctability, and an asymptotic distribution-free

property ensured by Wilks’ theorem. In the literature on nonparametric regression and RDD analysis, EL-based inferences via local linear smoothers primarily fall into two categories. One type of approach is based on undersmoothing, where the smoothing bandwidth  $h$  is chosen to be smaller than the optimal value such that the bias becomes asymptotically negligible relative to the variance; see, e.g., [Chen and Qin \(2000\)](#), [Otsu \(2012\)](#) and [Otsu et al. \(2015\)](#). The other approach relies on bias correction techniques, which involve a pilot bandwidth  $b$  to estimate and remove the asymptotic bias. Examples include applications to varying-coefficient and semiparametric models with longitudinal data ([Xue and Zhu; 2007a,b](#)), functional concurrent linear models ([Wang et al.; 2018](#)) and RDD ([Ma and Yu; 2020](#)).

Nevertheless, both approaches raise practical concerns. Undersmoothing, while producing valid coverage asymptotically, often results in increased variance and overly wide confidence intervals, leading to reduced efficiency in finite samples. Bias correction, on the other hand, requires the correction term to be first-order negligible to guarantee that Wilks’ theorem holds. To examine these issues, we investigate, in [Section 2](#), two conventional bias-corrected EL methods in nonparametric regression, where the bias estimators are built upon Taylor expansion and direct differencing, respectively. Under mild regularity conditions, we establish that the asymptotic distributions of the resulting EL ratios depend explicitly on the ratio  $h/b$ . Specifically, the standard chi-squared limiting distribution holds only when  $h/b \rightarrow 0$  as  $n \rightarrow \infty$ ; otherwise, the Wilks’ phenomenon fails. However, such a ratio condition is often violated in practice, as noted by [Calonico et al. \(2014\)](#). For example, the analysis of Brazilian mayoral election data in [Section 6](#) selects optimal bandwidths  $h = 15.287$  and  $b = 27.523$ , yielding a ratio of  $h/b = 0.55$ , which is not sufficiently small to guarantee convergence to zero. Likewise, the aforementioned papers on bias correction do not satisfy  $h/b \rightarrow 0$ , resulting in asymptotic distributions of their EL ratios that deviate from the standard chi-squared limit. Consequently, the coverage probabilities based on conventional bias-corrected EL procedures and standard chi-squared cut-offs often fall below nominal

levels, as further demonstrated in Section 5 through extensive simulations. Recognizing a similar pattern in RDD settings, [Ma and Yu \(2020\)](#) proposed a scale-adjusted EL ratio to restore the pivotal property asymptotically. Although sometimes effective, the scale factor depends on the estimation of the variance and covariance of the local linear estimates and the estimated bias, making it cumbersome to implement and diminishing the distribution-free appeal of EL. Therefore, generalizing the bias-corrected EL inference method to properly address the non-negligible first-order impact of the estimated bias under practically reasonable and more general conditions remains a non-trivial task, and no satisfactory solution has yet been established in the literature.

To tackle this challenge, we propose a novel bias-corrected EL framework, called robust EL, that delivers valid confidence intervals across a wider range of bandwidth selections for nonparametric regression and RDD. Unlike existing methods, which typically handle first-order impact by adjusting EL ratios, our proposal adopts a fundamentally different strategy by developing new sets of weights, termed “robust weights”, which simultaneously achieve bias correction and account for the additional variability introduced by the bias estimation in the EL formulation. Building on the new weighting schemes in Section 3.1, we propose two types of robust EL ratio functions and demonstrate that, under standard regularity conditions in nonparametric regression, both robust EL ratios converge to a standard chi-squared distribution within the refined asymptotic framework of [Calonico et al. \(2014\)](#), where the ratio

$$\frac{h}{b} \rightarrow \kappa \in [0, 1], \text{ as } n \rightarrow \infty. \quad (1)$$

In fact, the term “robust” in our proposal is inspired by the robust bias correction framework of [Calonico et al. \(2014\)](#). While our method can also be described as robust weighted EL or robust bias-corrected EL, we refer to it simply as robust EL for brevity. We further extend the robust EL approaches to accommodate both sharp and fuzzy RDD settings, establishing the corresponding versions of Wilks’ Theorem in this context. Numerical studies confirm that

our methods consistently outperform the original EL based on undersmoothing, conventional bias-corrected EL procedures, and the normal approximation-based approach of [Calonico et al. \(2014\)](#), particularly in terms of empirical size and coverage probabilities.

Our paper makes three main contributions. On the method side, we pioneer the development of a simple yet valid framework for bias-corrected EL inferences based on the construction of fully data-adaptive robust weights in nonparametric regression. Our proposal jointly corrects bias and addresses its variability, further enabling a single-pass computation of robust confidence intervals while eliminating the need for complex variance estimation. Importantly, our method preserves the distribution-free nature of EL, allowing confidence intervals to be constructed using standard chi-squared critical values. On the theory side, we investigate the asymptotic distributions of both conventional and robust EL-based inference procedures under different bandwidth regimes for the ratio  $h/b$ . A key result establishes that conventional bias-corrected EL methods fail to satisfy the standard chi-squared limiting distribution unless  $h/b \rightarrow 0$ , whereas our robust EL approaches restore Wilks' theorem under the more general ratio condition in (1). This, in turn, implies that our methods ensure valid inference without requiring undersmoothing and remain robust to choices of  $h$  and  $b$ , thereby facilitating a more flexible bandwidth selection in practice. Extensive simulation studies in Section 5 further confirm the superior finite-sample performance of our robust EL methods.

On the application side, we show that the proposed robust EL procedure and the associated theory can be seamlessly extended to both sharp and fuzzy RDD settings by adapting the robust weights and EL constraints accordingly. Under some additional conditions, the pivotal property continues to hold asymptotically. Beyond RDD, our robust EL framework is potentially applicable to a broader range of nonparametric and semiparametric models, including those considered in [Xu \(2013, 2020\)](#), [Chiang et al. \(2019\)](#), [Qu and Yoon \(2019\)](#), and [Dong et al. \(2023\)](#). It is worth noting that [Calonico et al. \(2014, 2018\)](#) made significant contributions to robust inference in RDD analysis. Specifically, they developed a robust bias-corrected inference procedure based on normal approximation, which handles the po-

tential first-order impact of the bias estimator within the refined asymptotic framework in (1). However, as highlighted by Otsu et al. (2015), their approach requires estimating the asymptotic variance of the bias correction term, which is complicated due to the discontinuities in the conditional mean, variance, and covariance functions, and involves additional nonparametric regressions. In contrast, our robust EL procedure is fully automatic and thus provides a simpler and effective alternative to the literature.

The rest of the paper is organized as follows. In Section 2, we discuss the limitations of original and conventional bias-corrected EL methods in nonparametric regression. Section 3 presents the construction of robust weights and details our proposed robust EL approaches, along with their asymptotic distributions. In Section 4, we apply our proposal to both sharp and fuzzy RDD and establish the corresponding theoretical validity. Sections 5 and 6 illustrate the superiority of our robust EL approaches over the original and conventional bias-corrected EL approaches through extensive simulation studies and the analysis of two real datasets, respectively. Section 7 concludes the paper and discusses several extensions. All technical proofs are relegated to the supplementary material.

## 2 Pitfalls of conventional EL methods

To facilitate the construction of our robust confidence intervals for nonparametric regression, we start with an overview of local polynomial estimation and the original EL-based inference procedure of Chen and Qin (2000) in Section 2.1, and present two conventional attempts at bias-corrected EL-based inference with asymptotic analysis in Section 2.2.

## 2.1 Methodological background

Suppose we observe  $\{(X_i, Y_i)\}_{i=1}^n$ , a set of  $n$  independent pairs from the nonparametric regression model,

$$Y_i = m(X_i) + \varepsilon_i, \quad i = 1, \dots, n, \quad (2)$$

where  $X_i$  follows a density function  $f(\cdot)$  with bounded support  $[0, 1]$ , and  $\{\varepsilon_i\}$  is a sequence of independent errors satisfying  $E(\varepsilon_i|X_i = x) = 0$  and  $\sigma^2(x) = E(\varepsilon_i^2|X_i = x) < \infty$ . In what follows, denote  $K_h(\cdot) = K(\cdot/h)/h$  for a univariate kernel  $K$  with bandwidth  $h > 0$ . We define the design matrix of order  $p$  as

$$\mathbf{X}_{p,h} = \begin{pmatrix} 1 & \frac{X_1-x}{h} & \dots & \left(\frac{X_1-x}{h}\right)^p \\ \vdots & \vdots & & \vdots \\ 1 & \frac{X_n-x}{h} & \dots & \left(\frac{X_n-x}{h}\right)^p \end{pmatrix} \in \mathbb{R}^{n \times (p+1)}.$$

Let  $\mathbf{W}_h = \text{diag}\{K_h(X_i - x)\}$  be the  $n \times n$  diagonal matrix of kernel weights. We write  $S_{j,h}(x) = n^{-1} \sum_{i=1}^n K_h(X_i - x)(X_i - x)^j/h^j$ , and put  $\mathbf{S}_{p,h} = n^{-1} \mathbf{X}_{p,h}^\top \mathbf{W}_h \mathbf{X}_{p,h}$ , whose  $(j, k)$ -th entry is given by  $S_{j+k-2,h}$  for  $j, k = 1, \dots, p+1$ .

The local polynomial estimator of order  $p$  for the  $\ell$ -th derivative  $m^{(\ell)}(x)$  with bandwidth  $h$ , denoted as  $\widehat{m}_{p,h}^{(\ell)}(x)$ , at each  $x \in [0, 1]$ , takes the form of

$$\widehat{m}_{p,h}^{(\ell)}(x) = \ell!(nh^\ell)^{-1} \mathbf{e}_{\ell+1}^\top \mathbf{S}_{p,h}^{-1} \mathbf{X}_{p,h}^\top \mathbf{W}_h \mathbf{y} = \frac{\ell!}{nh^\ell} \sum_{i=1}^n W_{i,\ell,p,h}(x) Y_i, \quad \ell = 0, \dots, p,$$

where  $\mathbf{e}_{\ell+1} = (0, \dots, 0, 1, 0, \dots, 0)^\top$  is a unit vector with the 1 in the  $(\ell+1)$ -th position,  $\mathbf{y} = (Y_1, \dots, Y_n)^\top$ , and  $W_{i,\ell,p,h}(x) = \mathbf{e}_{\ell+1}^\top \mathbf{S}_{p,h}^{-1} \{1, (X_i - x)/h, \dots, (X_i - x)^p/h^p\}^\top K_h(X_i - x)$  for  $i = 1, \dots, n$ . We define the local linear weights as  $W_{i,h}(x) = K_h(X_i - x) \{S_{2,h}(x) - S_{1,h}(x)(X_i - x)/h\}$ . In the special case of  $\ell = 0$ , the local linear estimator of  $m(x)$  with bandwidth  $h$  then simplifies to

$$\widehat{m}_{1,h}(x) = \frac{1}{n} \sum_{i=1}^n W_{i,0,1,h}(x) Y_i = \frac{\sum_{i=1}^n W_{i,h}(x) Y_i}{\sum_{i=1}^n W_{i,h}(x)}.$$

Note that  $\widehat{m}_{1,h}(x)$  satisfies the weighted moment equation  $\sum_{i=1}^n W_{i,h}(x) (Y_i - \theta) = 0$ . Inspired

by this, [Chen and Qin \(2000\)](#) (referred to as CQ) introduced the original empirical log-likelihood ratio for  $m(x)$ , given by

$$l_{\text{CQ}}(\theta) = -2 \max \left\{ \sum_{i=1}^n \log(np_i) \left| p_i \geq 0, \sum_{i=1}^n p_i = 1, \sum_{i=1}^n p_i W_{i,h}(x)(Y_i - \theta) = 0 \right. \right\}.$$

However, this EL-based inference targets  $m(x) + \text{bias}(x)$ , rather than  $m(x)$  itself. Under standard regularity conditions, [Chen and Qin \(2000\)](#) demonstrated that  $l_{\text{CQ}}(m(x))$  asymptotically follows a standard chi-square distribution with one degree of freedom, provided that  $nh^5 \rightarrow 0$  and  $m^{(2)}(x) \neq 0$ . Hence, undersmoothing is required to reduce the impact of bias in this formulation.

## 2.2 Two conventional bias-corrected EL methods

We modify the original EL-based inference procedure for  $m(x)$  by directly incorporating two commonly-used bias correction strategies. The first approach is motivated by the Taylor expansion of  $m(X_i)$  around  $x$ . Let  $r(X_i) = m(X_i) - m(x) - m^{(1)}(x)(X_i - x)$  denote the approximation error at  $X_i$ . Applying a second-order expansion, we can approximate this error as  $r(X_i) \approx m^{(2)}(x)(X_i - x)^2/2$ . Since the bias in  $\hat{m}_{1,h}(x)$  arises from  $r(X_i)$  near  $x$ , we consider a bias estimator as

$$\hat{r}_{1,b}(X_i) = \frac{1}{2} \hat{m}_{2,b}^{(2)}(x)(X_i - x)^2, \quad (3)$$

where  $\hat{m}_{2,b}^{(2)}(x) = 2 \sum_{i=1}^n W_{i,2,2,b}(x) Y_i / (nb^2)$  denotes the local quadratic estimator of  $m^{(2)}(x)$  with a pilot bandwidth  $b$ . See [Fan et al. \(1998\)](#) for a detailed discussion on bias correction in general nonparametric settings and [Calonico et al. \(2014\)](#) for its applications in RDD. The corresponding Taylor-expansion-based Bias-corrected (TB) empirical log-likelihood ratio for  $m(x)$  is then defined as

$$l_{\text{TB}}(\theta) = -2 \max \left\{ \sum_{i=1}^n \log(np_i) \left| p_i \geq 0, \sum_{i=1}^n p_i = 1, \sum_{i=1}^n p_i W_{i,h}(x) \{Y_i - \hat{r}_{1,b}(X_i) - \theta\} = 0 \right. \right\}. \quad (4)$$



The second bias-corrected approach is inspired by the direct difference  $m(X_i) - m(x)$ . Rather than relying on a Taylor expansion, we approximate the bias using the local difference estimation, i.e.,

$$\hat{r}_{2,b}(X_i) = \hat{m}_{2,b}(X_i) - \hat{m}_{2,b}(x),$$

where  $\hat{m}_{2,b}(x)$  represents the local quadratic estimator of  $m(x)$  with a pilot bandwidth  $b > 0$ . Substituting this into the EL formulation, we obtain the **D**ifference-based **B**ias-corrected (DB) empirical log-likelihood ratio, defined as

$$l_{\text{DB}}(\theta) = -2 \max \left\{ \sum_{i=1}^n \log(np_i) \left| p_i \geq 0, \sum_{i=1}^n p_i = 1, \sum_{i=1}^n p_i W_{i,h}(x) \{Y_i - \hat{r}_{2,b}(X_i) - \theta\} = 0 \right. \right\}. \quad (5)$$

In particular, when the estimated bias  $\hat{r}_{2,b}(X_i)$  is replaced by its counterpart based on local linear estimators with bandwidth  $h = b$ , i.e.,  $\hat{m}_{1,h}(X_i) - \hat{m}_{1,h}(x)$ , this reduces to the special case of the so-called residual-adjusted EL method proposed by [Xue and Zhu \(2007a,b\)](#) for longitudinal data. Despite the different forms of bias correction, our established [Theorem 1](#) below remains applicable to their case.

To investigate the theoretical properties, we impose some regularity conditions.

**Condition 1.**  $E(\varepsilon_i^4) < \infty$ .

**Condition 2.** (i) Both  $f(x)$ , the density function of  $X$ , and  $\sigma^2(x) = E(\varepsilon_i^2 | X_i = x)$  are continuous and bounded away from zero; (ii) The function  $m(\cdot)$  is thrice continuously differentiable in a neighborhood of  $x$ .

**Condition 3.** The kernel function  $K(\cdot)$  is a symmetric and bounded density function with support  $[-1, 1]$ .

**Condition 4.** As  $n \rightarrow \infty$ ,  $h \rightarrow 0$ ,  $b^2 \log n \rightarrow 0$ ,  $nh^5 b^2 \rightarrow 0$ ,  $nh^3 b^4 \rightarrow 0$ ,  $nh \rightarrow \infty$ , and  $n^{\epsilon-1} b \rightarrow \infty$  with  $1 < \epsilon < 3/2$ .

Conditions 1–4 are standard in the nonparametric regression literature, see, e.g., [Fan and Zhang \(1999\)](#); [Chen and Qin \(2000\)](#); [Calonico et al. \(2014\)](#). The smoothness requirement on  $m(\cdot)$  in Condition 2 can be relaxed to being twice continuously differentiable, in which case the leading bias term reduces to  $o(h^2)$  instead of  $O(h^3)$ . For simplicity in our proofs, we choose to adopt the stronger condition here. The requirements  $nh^5b^2 \rightarrow 0$  and  $nh^3b^4 \rightarrow 0$  in Condition 4 ensure that both bias-correction terms are asymptotically unbiased.

Before presenting the theoretical results, we introduce a refined asymptotic framework that characterizes a more flexible and practically reasonable relationship between the smoothing bandwidth  $h$  and the pilot bandwidth  $b$ . For local polynomial estimation, balancing bias and variance typically results in the optimal bandwidth selections  $h \asymp n^{-1/5}$  for  $\hat{m}_{1,h}(x)$  and  $b \asymp n^{-1/7}$  for  $\hat{m}_{2,b}^{(2)}(x)$ . Given these rates, it is generally accepted in the literature to assume that the ratio  $h/b \rightarrow 0$ . While this assumption is theoretically convenient, determining how small  $h/b$  should be in practice remains unclear. For instance, when  $h = 0.1$  and  $b = 0.3$ , the ratio  $1/3$  may not be sufficiently small to effectively reduce the first-order impact of the bias correction. Thus, we instead follow [Calonico et al. \(2014\)](#) and impose the refined asymptotic framework in (1). We now proceed to examine the asymptotic distributions of these two conventional bias-corrected EL ratio functions.

**Theorem 1.** *Suppose that Conditions 1–4 hold,  $m(x)$  is the true parameter, and  $x$  is an interior point.*

(a) *If  $h/b \rightarrow 0$  as  $n \rightarrow \infty$ , then,*

$$l_{\text{TB}} \{m(x)\} \xrightarrow{\mathcal{D}} \chi_1^2, \quad \text{and} \quad l_{\text{DB}} \{m(x)\} \xrightarrow{\mathcal{D}} \chi_1^2,$$

*as  $n \rightarrow \infty$ , where  $\xrightarrow{\mathcal{D}}$  means the convergence in distribution;*

(b) *If  $h/b \rightarrow \kappa \in (0, 1]$  as  $n \rightarrow \infty$ , then,*

$$l_{\text{TB}} \{m(x)\} \xrightarrow{\mathcal{D}} \gamma_{1,\kappa} \chi_1^2, \quad \text{and} \quad l_{\text{DB}} \{m(x)\} \xrightarrow{\mathcal{D}} \gamma_{2,\kappa} \chi_1^2,$$

as  $n \rightarrow \infty$ , where the constants  $\gamma_{1,\kappa}$  and  $\gamma_{2,\kappa}$  are specified in Section A.1 of the supplementary material with  $\gamma_{1,\kappa} \neq 1$  and  $\gamma_{2,\kappa} \neq 1$ .

**Remark 1.** *Theorem 1 highlights the critical role of the bandwidth ratio  $h/b$  in shaping the asymptotic properties of the conventional bias-corrected EL ratios. In particular, when  $\kappa \neq 0$ , these EL ratios asymptotically deviate from the standard chi-squared distribution. Instead, their limiting distributions depend on nuisance parameters, i.e.,  $\gamma_{1,\kappa} \neq 1$  and  $\gamma_{2,\kappa} \neq 1$ , which complicates their use in inference. If ignored, hypothesis tests based on the standard  $\chi_1^2$  distribution may substantially over-reject true null hypotheses, leading to inflated Type I error rates. Likewise, the corresponding confidence intervals fall short of their nominal coverage levels, resulting in invalid inference conclusions. Alternatively, one might consider estimating  $\gamma_{1,\kappa}$  or  $\gamma_{2,\kappa}$  and applying a scaled chi-squared distribution to correct the inference procedure. However, such an adjustment not only increases the implementation complexity but, more importantly, disrupts the distribution-free property of empirical likelihood, making it a less desirable solution in both theory and practice.*

**Remark 2.** *While Theorem 1 focuses on the case where  $x$  lies in the interior of the support, a similar result holds when  $x$  is near the boundary. The discussion in Remark 1 then naturally extends to the RDD analysis, where inference at the cutoff is of primary interest. We will explore the RDD settings further in Section 4.*

The failure of Wilks' theorem when  $h/b \rightarrow \kappa \in (0, 1]$  can be explained as follows. Define  $Z_i(x) = W_{i,h}(x) \{Y_i - \hat{r}_{1,b}(X_i) - m(x)\}$ , and consider the following quantities:

$$U_1(x) = \frac{1}{n} \sum_{i=1}^n Z_i(x), \quad U_2(x) = \frac{1}{n} \sum_{i=1}^n \{Z_i(x)\}^2.$$

As shown in the supplemental material, we can establish that

$$l_{\text{TB}}\{m(x)\} = \{U_2(x)\}^{-1} \{U_1(x)\}^2 \{1 + o_P(1)\}.$$

The key insight is that while deriving the limiting distribution of  $U_1(x)$  requires accounting for the additional variability introduced by the bias estimator  $\hat{r}_{1,b}(X_i)$ , the convergence in

probability of  $U_2(x)$  depends only on the consistency of the local quadratic estimator  $\hat{m}_{2,b}^{(2)}(x)$  used in the bias estimation. This indicates that the conventional bias correction formulation incorporates only part of the additional variability, resulting in a scaled chi-squared limiting distribution. A similar limitation applies to  $l_{\text{DB}}\{m(x)\}$ . To address this issue, we propose a new strategy in Section 3 by constructing new weights to fully capture the variability associated with the bias estimators in a simple and effective way.

### 3 Methodology

In this section, we develop a new EL framework in the nonparametric regression setting, referred to as robust EL. We first propose two sets of robust weights in Section 3.1 and then construct the corresponding robust EL-based confidence intervals for  $m(x)$  with theoretical validity in Section 3.2.

#### 3.1 Construction of robust weights

We begin by revisiting equation (4). Recall that

$$\hat{m}_{2,b}^{(2)}(x) = \frac{2}{nb^2} \sum_{i=1}^n W_{i,2,2,b}(x) Y_i = \frac{2}{b^2} \sum_{i=1}^n \frac{1}{n} W_{i,2,2,b}(x) (Y_i - \theta),$$

where the last equality follows from the fact that  $\sum_{i=1}^n W_{i,2,2,b}(x) = 0$ . To fully incorporate the variability of the bias estimator into the EL formulation, we define a ‘weighted’ version of  $\hat{m}_{2,b}^{(2)}(x)$  as

$$\hat{m}_{2,b}^{(2)*}(x) = \frac{2}{b^2} \sum_{i=1}^n p_i W_{i,2,2,b}(x) (Y_i - \theta),$$

where we use weights  $\{p_i\}_{i=1}^n$  instead of  $n^{-1}$ . Substituting  $\hat{m}_{2,b}^{(2)}(x)$  in (3) with  $\hat{m}_{2,b}^{(2)*}(x)$  and rewriting the moment constraint in (4), we obtain that

$$\begin{aligned}
& \sum_{i=1}^n p_i W_{i,h}(x) \left\{ Y_i - \frac{1}{2} \widehat{m}_{2,b}^{(2)*}(x) (X_i - x)^2 - \theta \right\} \\
&= \sum_{i=1}^n p_i \left\{ W_{i,h}(x) - W_{i,2,2,b}(x) \frac{1}{b^2} \sum_{k=1}^n p_k W_{k,h}(x) (X_k - x)^2 \right\} (Y_i - \theta) \\
&= \sum_{i=1}^n p_i \left[ W_{i,h}(x) - W_{i,2,2,b}(x) \frac{1}{nb^2} \sum_{k=1}^n W_{k,h}(x) (X_k - x)^2 \{1 + o_P(1)\} \right] (Y_i - \theta),
\end{aligned}$$

where the second equality follows from the approximation

$$\frac{1}{b^2} \sum_{k=1}^n p_k W_{k,h}(x) (X_k - x)^2 = \frac{1}{nb^2} \sum_{k=1}^n W_{k,h}(x) (X_k - x)^2 \{1 + o_P(1)\}.$$

Therefore, instead of relying on both original weights  $\{W_{i,h}(x)\}_{i=1}^n$  and the bias estimators  $\{\widehat{r}_{1,b}(X_i)\}_{i=1}^n$  in (4), we introduce the Taylor-expansion-based *robust weights*  $\{W_{i,h,b}^*(x)\}_{i=1}^n$  :

$$W_{i,h,b}^*(x) = W_{i,h}(x) - W_{i,2,2,b}(x) \frac{1}{nb^2} \sum_{k=1}^n W_{k,h}(x) (X_k - x)^2, \quad (6)$$

which are fully data-adaptive and better equipped to handle the previously unaddressed uncertainty of  $\widehat{r}_{1,b}(X_i)$ . Some standard calculations yield that

$$\frac{1}{nb^2} \sum_{k=1}^n W_{k,h}(x) (X_k - x)^2 = O_P(\kappa_n^2) \quad \text{with} \quad \kappa_n = h/b.$$

If  $\kappa_n \rightarrow 0$ , then  $W_{i,h,b}^*(x) - W_{i,h}(x) = o_P(1)$ , implying that the robust weights asymptotically align with the original ones. However, if  $\kappa_n$  approaches a positive constant, then  $W_{i,h,b}^*(x) - W_{i,h}(x) = O_P(1)$ , indicating a substantial difference between the robust and original weights. This distinction is crucial in ensuring that the robust bias-corrected EL-based inference procedure, which will be introduced in Section 3.2, remains both theoretically valid and practically reliable, even when  $h/b$  does not vanish. See Theorem 2 in Section 3.2 for further theoretical details.

The same principle can be applied to equation (5). Recall that

$$\widehat{m}_{2,b}(X_i) - \widehat{m}_{2,b}(x) = \frac{1}{n} \sum_{k=1}^n \{W_{k,0,2,b}(X_i) - W_{k,0,2,b}(x)\} (Y_k - \theta),$$

where the equality holds as  $\sum_{k=1}^n \{W_{k,0,2,b}(X_i) - W_{k,0,2,b}(x)\} = 0$ . We can write its weighted

version as

$$\widehat{m}_{2,b}^*(X_i) - \widehat{m}_{2,b}^*(x) = \sum_{k=1}^n p_k \{W_{k,0,2,b}(X_i) - W_{k,0,2,b}(x)\} (Y_k - \theta).$$

Replacing this weighted estimator in (5) and rewriting the moment constraint yields that

$$\begin{aligned} & \sum_{i=1}^n p_i W_{i,h}(x) [Y_i - \{\widehat{m}_{2,b}^*(X_i) - \widehat{m}_{2,b}^*(x)\} - \theta] \\ &= \sum_{i=1}^n p_i \left[ W_{i,h}(x) - \sum_{k=1}^n p_k W_{k,h}(x) \{W_{i,0,2,b}(X_k) - W_{i,0,2,b}(x)\} \right] (Y_i - \theta) \\ &= \sum_{i=1}^n p_i \left[ W_{i,h}(x) - \frac{1}{n} \sum_{k=1}^n W_{k,h}(x) \{W_{i,0,2,b}(X_k) - W_{i,0,2,b}(x)\} \{1 + o_P(1)\} \right] (Y_i - \theta), \end{aligned}$$

where the second equality is due to

$$\sum_{k=1}^n p_k W_{k,h}(x) \{W_{i,0,2,b}(X_k) - W_{i,0,2,b}(x)\} = \frac{1}{n} \sum_{k=1}^n W_{k,h}(x) \{W_{i,0,2,b}(X_k) - W_{i,0,2,b}(x)\} \{1 + o_P(1)\}.$$

We then define the difference-based *robust weights*  $\{W_{i,h,b}^\circ(x)\}_{i=1}^n$  as

$$W_{i,h,b}^\circ(x) = W_{i,h}(x) - \frac{1}{n} \sum_{k=1}^n W_{k,h}(x) \{W_{i,0,2,b}(X_k) - W_{i,0,2,b}(x)\}, \quad (7)$$

which can also automatically adjust for the inherent variability of  $\widehat{r}_{2,b}(X_i)$  in (5). Similarly, when  $\kappa_n \rightarrow 0$ , the difference between the robust and original weights is negligible, i.e.,  $W_{i,h,b}^\circ(x) - W_{i,h}(x) = o_P(1)$ . When  $\kappa_n$  tends to a positive constant  $\kappa$ , then  $W_{i,h,b}^\circ(x) - W_{i,h}(x) = O_P(1)$ . It is worth noting that our numerical experiments demonstrate the superior performance of the robust weights in (7) over their local linear counterparts, where  $W_{i,0,2,b}(X_k)$  and  $W_{i,0,2,b}(x)$  are replaced by  $W_{i,0,1,b}(X_k)$  and  $W_{i,0,1,b}(x)$ , respectively. We thus adopt the local quadratic formulation in subsequent analysis.

## 3.2 Robust empirical likelihood

Building on the robust weights constructed in Section 3.1, we propose two refined versions of the bias-corrected empirical log-likelihood ratios for  $m(x)$  in model (2). To be specific, the **T**aylor-expansion-based **R**obust EL ratio and **D**ifference-based **R**obust EL ratio are

respectively given by

$$l_{\text{TR}}(\theta) = -2 \max \left\{ \sum_{i=1}^n \log(np_i) \mid p_i \geq 0, \sum_{i=1}^n p_i = 1, \sum_{i=1}^n p_i W_{i,h,b}^*(x)(Y_i - \theta) = 0 \right\},$$

$$l_{\text{DR}}(\theta) = -2 \max \left\{ \sum_{i=1}^n \log(np_i) \mid p_i \geq 0, \sum_{i=1}^n p_i = 1, \sum_{i=1}^n p_i W_{i,h,b}^\diamond(x)(Y_i - \theta) = 0 \right\},$$

where  $W_{i,h,b}^*(x)$  is defined in (6) and  $W_{i,h,b}^\diamond(x)$  is specified in (7). Before presenting their limiting distributions, we impose the refined asymptotic framework formally in Condition 5.

**Condition 5.** *The bandwidth  $h$  and the pilot bandwidth  $b$  satisfy*

$$\frac{h}{b} \rightarrow \kappa \in [0, 1], \text{ as } n \rightarrow \infty.$$

**Theorem 2.** *Assume that Conditions 1–5 hold,  $m^{(2)}(x) \neq 0$  and  $x$  is an interior point. Then, as  $n \rightarrow \infty$ ,*

$$l_{\text{TR}} \{m(x)\} \xrightarrow{\mathcal{D}} \chi_1^2, \quad \text{and} \quad l_{\text{DR}} \{m(x)\} \xrightarrow{\mathcal{D}} \chi_1^2.$$

Unlike the conventional bias-corrected EL ratios in Section 2.2, Theorem 2 demonstrates that the proposed  $l_{\text{TR}}$  and  $l_{\text{DR}}$  asymptotically follow  $\chi_1^2$  even when the bandwidth ratio  $h/b$  converges to a positive constant, ensuring the validity of the proposed robust EL methods. This highlights that the robust weighting schemes in (6) and (7) can internally adjust for the additional variability from bias correction, thus allowing for simple-yet-robust EL formulations that preserve the pivotal asymptotic properties across a broader range of bandwidth choices. Supported by Theorem 2, we construct the robust EL confidence interval for  $m(x)$  at the confidence level  $1 - \alpha$  as

$$I_{\alpha, \text{TR}} = \{\theta : l_{\text{TR}}(\theta) \leq \chi_1^2(\alpha)\}, \quad \text{or} \quad I_{\alpha, \text{DR}} = \{\theta : l_{\text{DR}}(\theta) \leq \chi_1^2(\alpha)\},$$

where  $\chi_1^2(\alpha)$  represents the upper  $\alpha$ -quantile of the  $\chi_1^2$ -distribution.

## 4 Regression discontinuity designs

We are now ready to apply our proposed EL-based inference framework to RDD analysis. Our goal is to develop a robust inference procedure for the regression discontinuity (RD) average treatment effect at the cutoff. Following the methodological framework in Section 3, we first introduce new weights and robust EL ratios for two main RDD settings, i.e., sharp and fuzzy RDD, in Sections 4.1 and 4.2, respectively. We then establish the limiting distributions and based on which construct the corresponding EL-based confidence intervals in Section 4.3.

### 4.1 Sharp RDD

In the canonical sharp RDD, we consider a random sample  $\{(Y_i(0), Y_i(1), X_i), i = 1, \dots, n\}$  drawn from the joint distribution of the triplet  $(Y(0), Y(1), X)$ . The covariate  $X_i$ , often referred to as the running or forcing variable, determines whether unit  $i$  receives the treatment ( $X_i \geq c$ ) or not ( $X_i < c$ ). For simplicity, we set the cutoff point  $c = 0$  without loss of generality. The random variables  $Y_i(1)$  and  $Y_i(0)$  denote the potential outcomes for unit  $i$  under treatment and control, respectively. In practice, we observe the random sample  $\{(Y_i, X_i), i = 1, \dots, n\}$ , where the observed outcome  $Y_i$  for each unit  $i$  is given by:

$$Y_i = (1 - T_i)Y_i(0) + T_iY_i(1),$$

with  $T_i = I(X_i \geq 0)$  indicating treatment receipt and  $I(\cdot)$  denoting the indicator function. Given that the conditional expectation functions  $E\{Y_i(1) | X = x\}$  and  $E\{Y_i(0) | X = x\}$  are continuous at  $x = 0$ , the sharp RD average treatment effect at the cutoff is identified as:

$$\tau_S \equiv E\{Y_i(1) - Y_i(0) | X = 0\} = \lim_{x \rightarrow 0^+} E(Y_i | X_i = x) - \lim_{x \rightarrow 0^-} E(Y_i | X_i = x).$$

Write  $\mu(x) = E(Y_i | X_i = x)$ ,  $\mu_+ = \lim_{x \rightarrow 0^+} \mu(x)$  and  $\mu_- = \lim_{x \rightarrow 0^-} \mu(x)$ . Then  $\tau_S = \mu_+ - \mu_-$ . The problem can thus be reframed as inferring the difference between the regression functions of the outcome, given the running variable, at the cutoff for the control and treated groups.



We now introduce the local linear weights for treated and control units, respectively,

$$W_{i,h}^+ = T_i K_h(X_i) \left( S_{2,h}^+ - S_{1,h}^+ \frac{X_i}{h} \right), \quad S_{j,h}^+ = \frac{1}{n} \sum_{i=1}^n T_i K_h(X_i) \left( \frac{X_i}{h} \right)^j,$$

$$W_{i,h}^- = (1 - T_i) K_h(X_i) \left( S_{2,h}^- - S_{1,h}^- \frac{X_i}{h} \right), \quad S_{j,h}^- = \frac{1}{n} \sum_{i=1}^n (1 - T_i) K_h(X_i) \left( \frac{X_i}{h} \right)^j.$$

Let  $\mathbf{Z}_i(\theta, a) = (W_{i,h}^+(Y_i - \theta - a), W_{i,h}^-(Y_i - a))^T$ . The original empirical log-likelihood function, introduced by [Otsu et al. \(2015\)](#), is given by

$$l_S(\theta, a) = -2 \max \left\{ \sum_{i=1}^n \log(np_i) \mid p_i \geq 0, \sum_{i=1}^n p_i = 1, \sum_{i=1}^n p_i \mathbf{Z}_i(\theta, a) = 0 \right\}.$$

and the corresponding empirical log-likelihood ratio for  $\tau_S$  is defined as

$$l_S(\theta) = \inf_{a \in \mathcal{A}} l_S(\theta, a),$$

where  $\mathcal{A}$  is the compact parameter space for  $a$ .

To implement the proposed robust EL approach, we employ a pilot bandwidth  $b$  and introduce  $W_{i,2,2,b}^+$  and  $W_{i,2,2,b}^-$  as counterparts of  $W_{i,2,2,b}(0)$ , computed using the subsamples  $\{i : T_i = 1\}$  and  $\{i : T_i = 0\}$ , respectively. Inspired by the robust weights introduced in [Section 3.1](#), for  $i = 1, \dots, n$ , we define

$$W_{i,h,b}^{\star+} = W_{i,h}^+ - n^{-1} b^{-2} W_{i,2,2,b}^+ \sum_{k=1}^n W_{k,h}^+ X_k^2, \quad W_{i,h,b}^{\star-} = W_{i,h}^- - n^{-1} b^{-2} W_{i,2,2,b}^- \sum_{k=1}^n W_{k,h}^- X_k^2,$$

and write

$$\mathbf{Z}_i^*(\theta, a) = (W_{i,h,b}^{\star+}(Y_i - \theta - a), W_{i,h,b}^{\star-}(Y_i - a))^T.$$

We then propose the Taylor-expansion-based robust empirical log-likelihood function

$$l_{S,TR}(\theta, a) = -2 \max \left\{ \sum_{i=1}^n \log(np_i) \mid p_i \geq 0, \sum_{i=1}^n p_i = 1, \sum_{i=1}^n p_i \mathbf{Z}_i^*(\theta, a) = 0 \right\}, \quad (8)$$

and the corresponding robust empirical log-likelihood ratio for  $\tau_S$  as

$$l_{S,TR}(\theta) = \inf_{a \in \mathcal{A}} l_{S,TR}(\theta, a). \quad (9)$$

To compute (9), we employ the Lagrange multiplier method, yielding

$$l_{\text{S,TR}}(\theta) = 2 \sum_{i=1}^n \log \{1 + \boldsymbol{\lambda}^{\text{T}} \mathbf{Z}_i^*(\theta, a)\}, \quad (10)$$

where  $\boldsymbol{\lambda}$  and  $a$  are determined by

$$\sum_{i=1}^n \frac{\mathbf{Z}_i^*(\theta, a)}{1 + \boldsymbol{\lambda}^{\text{T}} \mathbf{Z}_i^*(\theta, a)} = 0 \quad \text{and} \quad \sum_{i=1}^n \frac{\boldsymbol{\lambda}^{\text{T}} \mathbf{W}_i^*}{1 + \boldsymbol{\lambda}^{\text{T}} \mathbf{Z}_i^*(\theta, a)} = 0, \quad (11)$$

with  $\mathbf{W}_i^* = (W_{i,h,b}^{*+}, W_{i,h,b}^{*-})^{\text{T}}$ . Consequently, these equations can be effectively solved using the Newton-Lagrange algorithm or nested algorithm, as discussed in Owen (2001).

Similarly, let  $W_{i,0,2,b}^+(x)$  and  $W_{i,0,2,b}^-(x)$  be counterparts of  $W_{i,0,2,b}(x)$  using the subsamples  $\{i : T_i = 1\}$  and  $\{i : T_i = 0\}$ , respectively, and write

$$\begin{aligned} W_{i,h,b}^{\diamond+} &= W_{i,h}^+ - n^{-1} \sum_{k=1}^n W_{k,h}^+ \{W_{i,0,2,b}^+(X_k) - W_{i,0,2,b}^+(0)\}, \\ W_{i,h,b}^{\diamond-} &= W_{i,h}^- - n^{-1} \sum_{k=1}^n W_{k,h}^- \{W_{i,0,2,b}^-(X_k) - W_{i,0,2,b}^-(0)\}. \end{aligned}$$

The difference-based robust empirical likelihood ratio for  $\tau_{\text{S}}$ , denoted as  $l_{\text{S,DR}}(\theta)$ , can be defined and computed analogously by replacing  $W_{i,h,b}^{*+}$  and  $W_{i,h,b}^{*-}$  in (8)–(11) with  $W_{i,h,b}^{\diamond+}$  and  $W_{i,h,b}^{\diamond-}$ , respectively.

**Remark 3.** Given the representation of  $W_{i,h,b}^{*+}$ , the bias-corrected local linear estimator  $\hat{\tau}_{\text{S}}$  for  $\tau_{\text{S}}$  can be expressed as  $\hat{\tau}_{\text{S}} = \hat{\mu}_+ - \hat{\mu}_-$ , where the estimators  $\hat{\mu}_+$  and  $\hat{\mu}_-$  satisfy the following moment equations:

$$\sum_{i=1}^n W_{i,h,b}^{*+} (Y_i - \hat{\mu}_+) = 0, \quad \sum_{i=1}^n W_{i,h,b}^{*-} (Y_i - \hat{\mu}_-) = 0.$$

Calonico et al. (2014) derived the asymptotic variance of  $\hat{\tau}_{\text{S}}$  and constructed the normal-approximation-based robust confidence intervals for  $\tau_{\text{S}}$ . However, the variance introduced in their work is complex and requires additional estimation. In contrast, our robust EL proposal provides a simpler and automatic alternative, yielding valid inference without the need for explicit variance estimation.

## 4.2 Fuzzy RDD

Unlike the sharp RDD, which assumes that treatment status  $T_i$  is fully assigned based on the forcing variable  $X_i$ , fuzzy RDD accommodates scenarios where  $X_i$  influences but does not completely determine the treatment assignment. Specifically, in a fuzzy RDD, the conditional probability of receiving treatment changes discontinuously at the cutoff point  $X_i = 0$ :

$$\lim_{x \rightarrow 0^+} P(T_i = 1 \mid X_i = x) \neq \lim_{x \rightarrow 0^-} P(T_i = 1 \mid X_i = x).$$

To formally describe this setting, we consider a random sample  $(Y_i(1), Y_i(0), T_i(1), T_i(0), X_i)$  for  $i = 1, \dots, n$  from the joint distribution of  $(Y(1), Y(0), T(1), T(0), X)$ , where the treatment status of unit  $i$  is determined by  $T_i = T_i(0)I(X_i < 0) + T_i(1)I(X_i \geq 0)$ , with  $T_i(0), T_i(1) \in \{0, 1\}$ . The observed data consist of the sample  $\{(Y_i, T_i, X_i), i = 1, \dots, n\}$ .

According to [Hahn et al. \(2001\)](#), under appropriate conditions, the average treatment effect at the cutoff in a fuzzy RDD is nonparametrically identified as

$$\tau_F = \frac{\lim_{x \rightarrow 0^+} E(Y_i \mid X_i = x) - \lim_{x \rightarrow 0^-} E(Y_i \mid X_i = x)}{\lim_{x \rightarrow 0^+} E(T_i \mid X_i = x) - \lim_{x \rightarrow 0^-} E(T_i \mid X_i = x)} \equiv \frac{\mu_{Y^+} - \mu_{Y^-}}{\mu_{T^+} - \mu_{T^-}}.$$

The original empirical log-likelihood ratio, proposed by [Otsu et al. \(2015\)](#), for  $\tau_F$  can then be formulated as

$$l_F(\theta) = \inf_{(a, b_+, b_-) \in \mathcal{A} \times [0, 1] \times [0, 1]} l_F(\theta, a, b_+, b_-),$$

where  $l_F(\theta, a, b_+, b_-)$  is defined as

$$l_F(\theta, a, b_+, b_-) = -2 \max \left\{ \sum_{i=1}^n \log(np_i) \mid \begin{aligned} & p_i \geq 0, \sum_{i=1}^n p_i = 1, \\ & \sum_{i=1}^n p_i W_{i,h}^+(Y_i - \theta b_+ - a) = 0, \sum_{i=1}^n p_i W_{i,h}^+(T_i - b_+) = 0, \\ & \sum_{i=1}^n p_i W_{i,h}^-(Y_i - \theta b_- - a) = 0, \sum_{i=1}^n p_i W_{i,h}^-(T_i - b_-) = 0 \end{aligned} \right\}.$$

Adopting the robust approach similar to that used in [Section 4.1](#), we replace  $W_{i,h}^+$  and  $W_{i,h}^-$  with their robust counterparts  $W_{i,h,b}^{*+}$  and  $W_{i,h,b}^{*-}$  and introduce the Taylor-expansion-based

robust empirical log-likelihood function:

$$l_{\text{F,TR}}(\theta, a, b_+, b_-) = -2 \max \left\{ \sum_{i=1}^n \log(np_i) \left| \begin{array}{l} p_i \geq 0, \sum_{i=1}^n p_i = 1, \\ \sum_{i=1}^n p_i W_{i,h,b}^{*+} (Y_i - \theta b_+ - a) = 0, \sum_{i=1}^n p_i W_{i,h,b}^{*+} (T_i - b_+) = 0, \\ \sum_{i=1}^n p_i W_{i,h,b}^{*-} (Y_i - \theta b_- - a) = 0, \sum_{i=1}^n p_i W_{i,h,b}^{*-} (T_i - b_-) = 0 \end{array} \right. \right\}. \quad (12)$$

The corresponding robust empirical log-likelihood ratio for  $\tau_{\text{F}}$  is then given by

$$l_{\text{F,TR}}(\theta) = \inf_{(a, b_+, b_-) \in \mathcal{A} \times [0,1] \times [0,1]} l_{\text{F,TR}}(\theta, a, b_+, b_-). \quad (13)$$

Let  $\tilde{\mathbf{Z}}_i^*(\theta, a) = (W_{i,h,b}^{*+} (Y_i - \theta T_i - a), W_{i,h,b}^{*-} (Y_i - \theta T_i - a))^{\text{T}}$ . We can reformulate (13) as

$$l_{\text{F,TR}}(\theta) = 2 \sum_{i=1}^n \log \{1 + \boldsymbol{\lambda}^{\text{T}} \tilde{\mathbf{Z}}_i^*(\theta, a)\}, \quad (14)$$

where the parameters  $\boldsymbol{\lambda}$  and  $a$  satisfy

$$\sum_{i=1}^n \frac{\tilde{\mathbf{Z}}_i^*(\theta, a)}{1 + \boldsymbol{\lambda}^{\text{T}} \tilde{\mathbf{Z}}_i^*(\theta, a)} = 0, \quad \text{and} \quad \sum_{i=1}^n \frac{\boldsymbol{\lambda}^{\text{T}} \mathbf{W}_i^*}{1 + \boldsymbol{\lambda}^{\text{T}} \tilde{\mathbf{Z}}_i^*(\theta, a)} = 0, \quad (15)$$

As a result, the computational algorithms that have been developed for the context of sharp RDD can be seamlessly applied to this scenario. Finally, substituting  $W_{i,h,b}^{*+}$  and  $W_{i,h,b}^{*-}$  in (12)–(15) with  $W_{i,h,b}^{\diamond+}$  and  $W_{i,h,b}^{\diamond-}$ , respectively, we can define and compute the difference-based robust empirical likelihood ratio  $l_{\text{F,DR}}(\theta)$  for  $\tau_{\text{F}}$ .

**Remark 4.** To study  $\tau_{\text{F}}$ , [Calonico et al. \(2014\)](#) investigated the bias-corrected local linear estimator  $\hat{\tau}_{\text{F}}$  for  $\tau_{\text{F}}$ , defined as:

$$\hat{\tau}_{\text{F}} = \frac{\hat{\mu}_{Y+} - \hat{\mu}_{Y-}}{\hat{\mu}_{T+} - \hat{\mu}_{T-}},$$

where the estimators  $\hat{\mu}_{Y+}$ ,  $\hat{\mu}_{Y-}$ ,  $\hat{\mu}_{T+}$  and  $\hat{\mu}_{T-}$  satisfy the following equations:

$$\begin{aligned} \sum_{i=1}^n W_{i,h,b}^{*+} (Y_i - \hat{\mu}_{Y+}) &= 0, & \sum_{i=1}^n W_{i,h,b}^{*-} (Y_i - \hat{\mu}_{Y-}) &= 0, \\ \sum_{i=1}^n W_{i,h,b}^{*+} (T_i - \hat{\mu}_{T+}) &= 0, & \sum_{i=1}^n W_{i,h,b}^{*-} (T_i - \hat{\mu}_{T-}) &= 0. \end{aligned}$$

While the estimator  $\hat{\tau}_{\text{F}}$  has an analytic form, its variance estimator relies on multiple Taylor

expansions and approximations, making it much more complex than the variance derivation and estimation required in the sharp RDD case. This further demonstrates a key advantage of our robust EL method, as it offers a unified framework for both RDD settings. Following similar arguments, our method can potentially be adapted to other RDD settings, such as kink RDD, which targets discontinuities in the first derivative of the regression function at the cutoff.

### 4.3 Asymptotic properties

We first impose some regularity conditions on the sharp RDD setting.

**Condition 6.** For some  $\rho_0 > 0$ , the following holds in the neighborhood  $(-\rho_0, \rho_0)$  around the cutoff  $x = 0$ :

- (i)  $E(Y_i^4|X_i = x) < \infty$ ;
- (ii) The density function  $f(x)$  of  $X$  is continuous and bounded away from zero;
- (iii)  $\mu_+(x) = E\{Y_i(1)|X_i = x\}$  and  $\mu_-(x) = E\{Y_i(0)|X_i = x\}$  are thrice continuously differentiable;
- (iv) The conditional variance  $\sigma^2(x) = \text{Var}(Y_i|X_i = x)$  is right and left continuous at the cutoff  $x = 0$  and bounded away from zero.

**Condition 7.**  $\mathcal{A}$  is compact and the true value  $\mu_-$  is an interior point of  $\mathcal{A}$ .

We then give an additional condition to address the fuzzy RDD setting.

**Condition 8.** From some  $\rho_0 > 0$ , the following holds in the neighborhood  $(-\rho_0, \rho_0)$  around the cutoff  $x = 0$ .

- (i)  $\mu_{T+}(x) = E\{T_i(1)|X_i = x\}$  and  $\mu_{T-}(x) = E\{T_i(0)|X_i = x\}$  are thrice continuously differentiable;

- (ii) *The conditional variance  $\sigma_T^2(x) = \text{Var}(T_i|X_i = x)$  is right and left continuous at  $x = 0$  and bounded away from zero.*

The above conditions are standard in the literature, with analogous assumptions imposed in [Calonico et al. \(2014\)](#) and [Otsu et al. \(2015\)](#). In particular, Conditions [6\(iii\)](#) and [8\(i\)](#) establish conventional smoothness requirements on the regression functions. These conditions play a pivotal role in governing the leading bias terms of the estimators in both settings. Furthermore, Conditions [6\(iv\)](#) and [8\(ii\)](#) place standard constraints on the conditional variance of the observed outcome and treatment, respectively, allowing for potential heterogeneity across the threshold.

**Theorem 3.** *Assume that Conditions [3–7](#) hold. Then, as  $n \rightarrow \infty$ ,*

$$l_{S,TR}(\tau_S) \xrightarrow{\mathcal{D}} \chi_1^2, \quad \text{and} \quad l_{S,DR}(\tau_S) \xrightarrow{\mathcal{D}} \chi_1^2.$$

**Theorem 4.** *Assume that Conditions [3–8](#) hold. Then, as  $n \rightarrow \infty$ ,*

$$l_{F,TR}(\tau_F) \xrightarrow{\mathcal{D}} \chi_1^2, \quad \text{and} \quad l_{F,DR}(\tau_F) \xrightarrow{\mathcal{D}} \chi_1^2.$$

Theorems [3](#) and [4](#) reveal that the proposed EL ratios for both sharp and fuzzy RDD settings converge asymptotically to  $\chi_1^2$ , which nicely justifies the construction of robust EL-based confidence intervals. For the sharp RDD setting, the confidence intervals for  $\tau_S$  at the confidence level  $1 - \alpha$  are respectively given by

$$I_{\alpha,TR}^{(S)} = \{\theta : l_{S,TR}(\theta) \leq \chi_1^2(\alpha)\}, \quad \text{and} \quad I_{\alpha,DR}^{(S)} = \{\theta : l_{S,DR}(\theta) \leq \chi_1^2(\alpha)\}.$$

For fuzzy RDD, the corresponding confidence intervals for  $\tau_F$  are defined as

$$I_{\alpha,TR}^{(F)} = \{\theta : l_{F,TR}(\theta) \leq \chi_1^2(\alpha)\}, \quad \text{and} \quad I_{\alpha,DR}^{(F)} = \{\theta : l_{F,DR}(\theta) \leq \chi_1^2(\alpha)\}.$$

## 5 Simulation studies

We conduct a series of simulations to illustrate the performance of our proposed robust EL inference methods. Sections [5.1](#) and [5.2](#) examine inference scenarios for  $m(x)$  and the

sharp RD effect  $\tau_S$ , respectively. In each scenario, we generate random samples  $(X_i, Y_i)$  for  $i = 1, \dots, n$  from (2), where the measurement locations  $X_i$  and errors  $\varepsilon_i$  are sampled independently from  $2\mathcal{B}(2, 4) - 1$ , with  $\mathcal{B}(\beta_1, \beta_2)$  denoting a beta distribution with shape parameters  $\beta_1$  and  $\beta_2$ , and the normal distribution  $\mathcal{N}(0, 0.1295^2)$ , respectively. The exact forms of  $m(x)$  will be specified in the respective sections. For simplicity, we use the Epanechnikov kernel to compute the empirical log-likelihood ratios.

## 5.1 Nonparametric regression

In this section, we consider the following two functional forms of  $m(x)$ , with a focus on inference at the point  $x = -0.5$ .

MODEL 1.  $m(x) = 0.25(x + 1)^2 - \sin(\pi x)$ .

MODEL 2.  $m(x) = 0.3 \exp\{-4(2x + 1)^2\} + 0.7 \exp\{-16(2x - 1)^2\}$ .

See also Figure S1 of the supplementary material for visualizations of  $m(x)$  and the evaluation points. For each model introduced above, we generate  $n \in \{500, 1000\}$  observations and replicate each simulation 1000 times. We compare the performance of the proposed Taylor-expansion-based **R**obust EL method (TR) and **D**ifference-based **R**obust EL method (DR) against their conventional Bias-Corrected counterparts (denoted as TB and DB, respectively) and the **O**riginal empirical likelihood method (Orig) introduced by Chen and Qin (2000). To examine their robustness to the choice of bandwidths, we consider  $h \in \{0.06, 0.08, \dots, 0.14\}$  for  $n = 500$  and  $h \in \{0.04, 0.06, \dots, 0.12\}$  for  $n = 1000$ , with two different pilot bandwidth settings  $b = 1.2h$  and  $b = 1.5h$ . Figure 1 reports empirical sizes for  $m(x)$  at its true value under the 5% nominal level and empirical interval coverages at the 95% confidence level for five comparison methods. Table 1 provides the corresponding average empirical interval lengths along with the empirical interval coverages. Since the results for Models 1 and 2 exhibit similar trends, we only present numerical results for Model 1 here and defer those for Model 2 to Figure S2 and Table S1 in the supplementary material.

Several conclusions can be drawn from Figures 1 and S2 and Tables 1 and S1. First, our proposed two robust methods (TR and DR) perform equally well, achieving the most accurate empirical sizes and coverages across all settings. This demonstrates the effectiveness of our approaches and their robustness to both  $h$  and  $b$ . Second, all other competing methods suffer from significant size and coverage distortions. As expected, the Orig method is highly sensitive to bandwidth selection, with its performance deteriorating severely when  $h$  becomes slightly larger. Meanwhile, both conventional methods (TB and DB) fail completely, as reflected by elevated empirical sizes and reduced empirical coverages across all values of  $h$ . This pattern provides strong validation for Theorem 1, which states that  $l_{\text{TB}}\{m(x)\}$  and  $l_{\text{DB}}\{m(x)\}$  deviate from  $\chi_1^2$  when the condition  $h/b \rightarrow 0$  is violated. Interestingly, their performance improves slightly when  $b = 1.5h$  compared to  $b = 1.2h$ , likely due to the smaller ratio  $h/b$  in the former case. Lastly, the average interval lengths decrease as  $h$  and  $n$  increase for all methods. This further highlights the advantage of our proposed robust methods, which can produce narrower confidence intervals while maintaining correct size and coverage for a given  $n$ , as evidenced by the bolded results. In contrast, the Orig method, constrained by the requirement for undersmoothing, results in wider intervals.

## 5.2 Regression discontinuity design

We now turn to the sharp RDD setting and investigate Model 3 below, constructed using data in Lee (2008) with  $\tau_S = 0.5$ , at the boundary point  $x = 0$ . A similar model can also be found in Imbens and Kalyanaraman (2012) and Calonico et al. (2014). Further analysis of a simple low-order polynomial function, termed Model 4, is provided in Section B of the supplementary material. See Figure S3 for the visualizations of  $m(x)$  for both models.

MODEL 3.

$$m(x) = \begin{cases} 0.3 + 1.27x + 7.18x^2 + 20.21x^3 + 21.54x^4 + 7.33x^5 & \text{if } x < 0, \\ 0.8 + 0.84x - 3.00x^2 + 7.99x^3 - 9.01x^4 + 3.56x^5 & \text{if } x \geq 0. \end{cases}$$



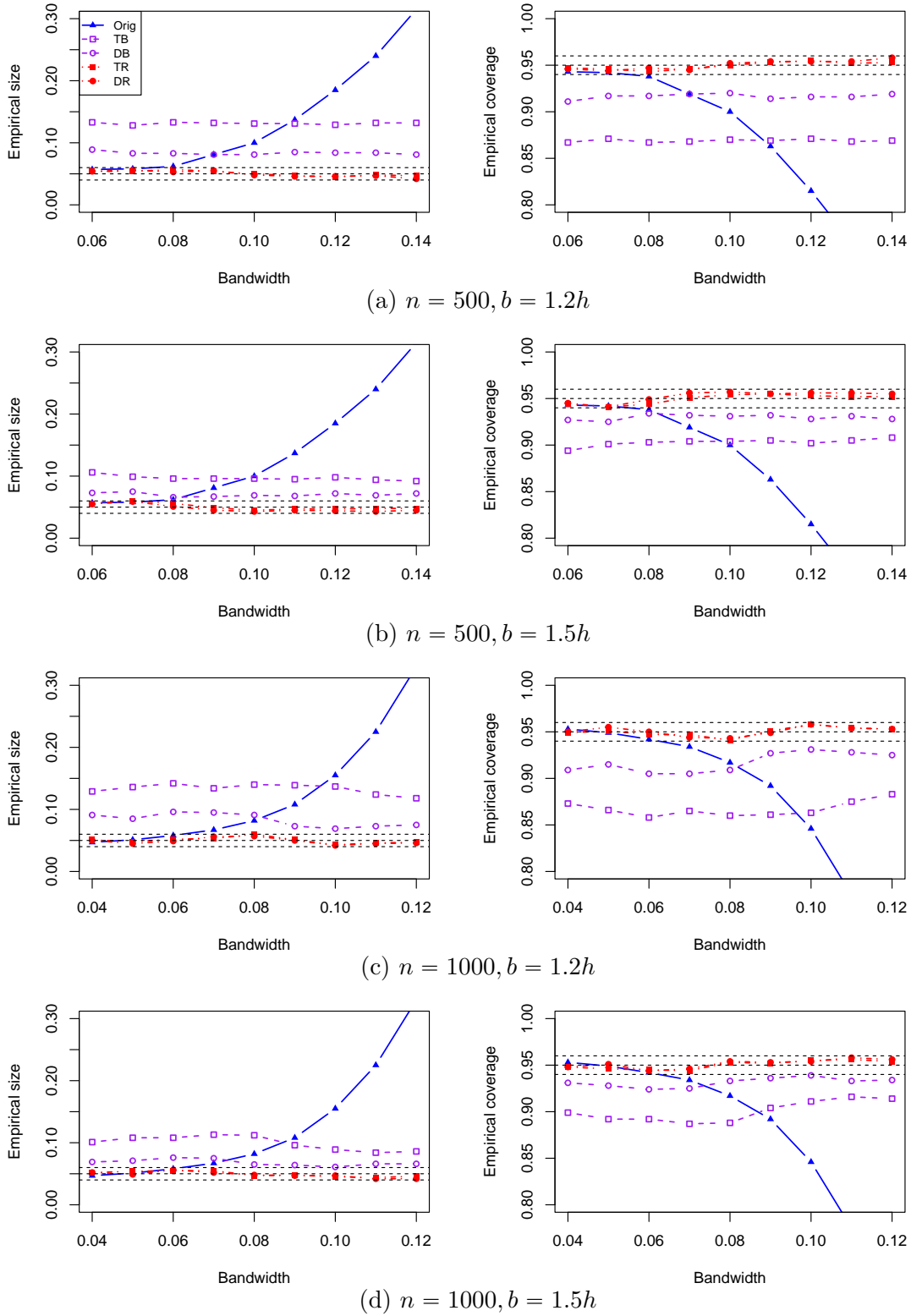


Figure 1: Plots of empirical sizes and empirical coverages as functions of bandwidth over 1000 simulation runs at  $x = -0.5$  for Model 1.

Table 1: Average interval lengths and empirical coverages (in parentheses) of 95% confidence intervals over 1000 simulation runs at  $x = -0.5$  for Model 1. The best performances, with empirical coverages close to 95% and short interval lengths, are in bold font.

$h$	$n = 500$					$n = 1000$				
	0.06	0.08	0.10	0.12	0.14	0.04	0.06	0.08	0.10	0.12
Orig	<b>0.071</b> <b>(0.943)</b>	0.062 (0.938)	0.055 (0.900)	0.050 (0.815)	0.047 (0.684)	0.061 (0.953)	<b>0.050</b> <b>(0.942)</b>	0.043 (0.917)	0.039 (0.846)	0.036 (0.671)
Setting: $b = 1.2h$										
TB	0.071 (0.867)	0.061 (0.867)	0.055 (0.870)	0.050 (0.871)	0.047 (0.869)	0.061 (0.873)	0.050 (0.858)	0.043 (0.860)	0.039 (0.863)	0.035 (0.883)
DB	0.071 (0.911)	0.061 (0.917)	0.055 (0.920)	0.050 (0.916)	0.046 (0.919)	0.061 (0.909)	0.050 (0.905)	0.043 (0.909)	0.039 (0.931)	0.035 (0.925)
TR	0.093 (0.947)	0.081 (0.943)	0.072 (0.950)	0.066 (0.955)	<b>0.062</b> <b>(0.953)</b>	0.080 (0.949)	0.066 (0.947)	0.057 (0.941)	0.051 (0.958)	<b>0.047</b> <b>(0.953)</b>
DR	0.098 (0.946)	0.085 (0.947)	0.076 (0.952)	0.070 (0.954)	<b>0.065</b> <b>(0.958)</b>	0.085 (0.950)	0.069 (0.950)	0.060 (0.943)	0.053 (0.958)	<b>0.049</b> <b>(0.953)</b>
Setting: $b = 1.5h$										
TB	0.071 (0.894)	0.061 (0.903)	0.055 (0.904)	0.050 (0.902)	0.047 (0.908)	0.061 (0.899)	0.050 (0.892)	0.043 (0.888)	0.039 (0.911)	0.035 (0.914)
DB	0.071 (0.927)	0.061 (0.934)	0.055 (0.931)	0.050 (0.928)	0.046 (0.928)	0.061 (0.931)	0.050 (0.924)	0.043 (0.933)	0.039 (0.939)	0.035 (0.934)
TR	0.085 (0.944)	0.074 (0.944)	0.066 (0.954)	0.061 (0.953)	<b>0.057</b> <b>(0.952)</b>	0.074 (0.948)	0.060 (0.945)	0.052 (0.953)	0.047 (0.955)	<b>0.043</b> <b>(0.954)</b>
DR	0.091 (0.945)	0.079 (0.949)	0.071 (0.957)	0.065 (0.956)	<b>0.061</b> <b>(0.955)</b>	0.078 (0.948)	0.064 (0.944)	0.055 (0.954)	0.050 (0.954)	<b>0.046</b> <b>(0.956)</b>

Similar to Section 5.1, we evaluate the performance of Orig, TB, DB, TR and DR methods under this sharp RDD setting. For comparison, we also include the asymptotic robust bias correction approach proposed by Calonico et al. (2014) (denoted as CCT). To assess the sensitivity of the competing methods to the bandwidth choices, Figure 2 displays the empirical sizes and empirical coverages based on 1000 simulations over  $h \in \{0.15, 0.18, \dots, 0.27\}$  for  $n = 500$  and  $h \in \{0.12, 0.18, \dots, 0.24\}$  for  $n = 1000$  under the settings  $b = 1.2h$  and  $b = 1.5h$ . Table 2 presents the corresponding average interval lengths and coverages. The results align with the findings in Section 5.1. In particular, we observe a similar size distortion effect for the Orig method as in Otsu et al. (2015). Overall, both TR and DR outperform CCT across the range of  $h$  values, delivering empirical sizes and coverages closer to the target levels while keeping average interval lengths comparable. For instance, when  $(n, h, b) = (1000, 0.21, 1.2h)$ , our proposed methods (TR and DR) achieve more than 94.6%

empirical coverage with interval lengths of 0.185 and 0.187, respectively, while CCT provides 93.9% coverage with an interval length of 0.19 under  $(n, h, b) = (1000, 0.18, 1.2h)$ . This pattern holds across other  $n$  and  $b$  settings.

We further adopt the MSE-optimal bandwidth selectors for  $h$  and  $b$  in [Calonico et al. \(2014\)](#) to investigate the effectiveness of the various inference methods under such data-driven bandwidths, denoted as  $\hat{h}_{\text{opt}}$  and  $\hat{b}_{\text{opt}}$ , respectively. Both the MSE-optimal bandwidth selection method and the CCT method introduced above are implemented using the R package `rdrobust`. [Table 3](#) provides numerical summaries for three different settings with  $(h, b) = (\hat{h}_{\text{opt}}, \hat{b}_{\text{opt}})$ ,  $(\hat{h}_{\text{opt}}, 1.2\hat{h}_{\text{opt}})$  and  $(\hat{h}_{\text{opt}}, 1.5\hat{h}_{\text{opt}})$  based on 10000 replications, including the empirical sizes for  $\tau_S = 0.5$  at 5% nominal level, empirical coverages at 95% confidence level and the average interval lengths. Also reported are the average bandwidth values for the selected  $h$  and  $b$  in each setting. A few trends are apparent. First, the Orig, TB and DB methods tend to significantly over-reject the null hypothesis, resulting in notable size and coverage errors. Second, the three robust methods demonstrate clear improvements in empirical sizes and coverages. Among them, DR performs the best, closely followed by TR, while CCT exhibits relatively inferior performance. This reaffirms the robustness and effectiveness of our proposed method in enhancing inference performance.

## 6 Real data analysis

In this section, we apply our proposed TR and DR methods to evaluate the sharp RD effects in two real-world social study examples. We also implement the Orig, TB, DB and CCT methods, as introduced in [Section 5](#). To ensure a fair comparison, the optimal bandwidths  $\hat{h}_{\text{opt}}$  and  $\hat{b}_{\text{opt}}$  are used across all competing methods.

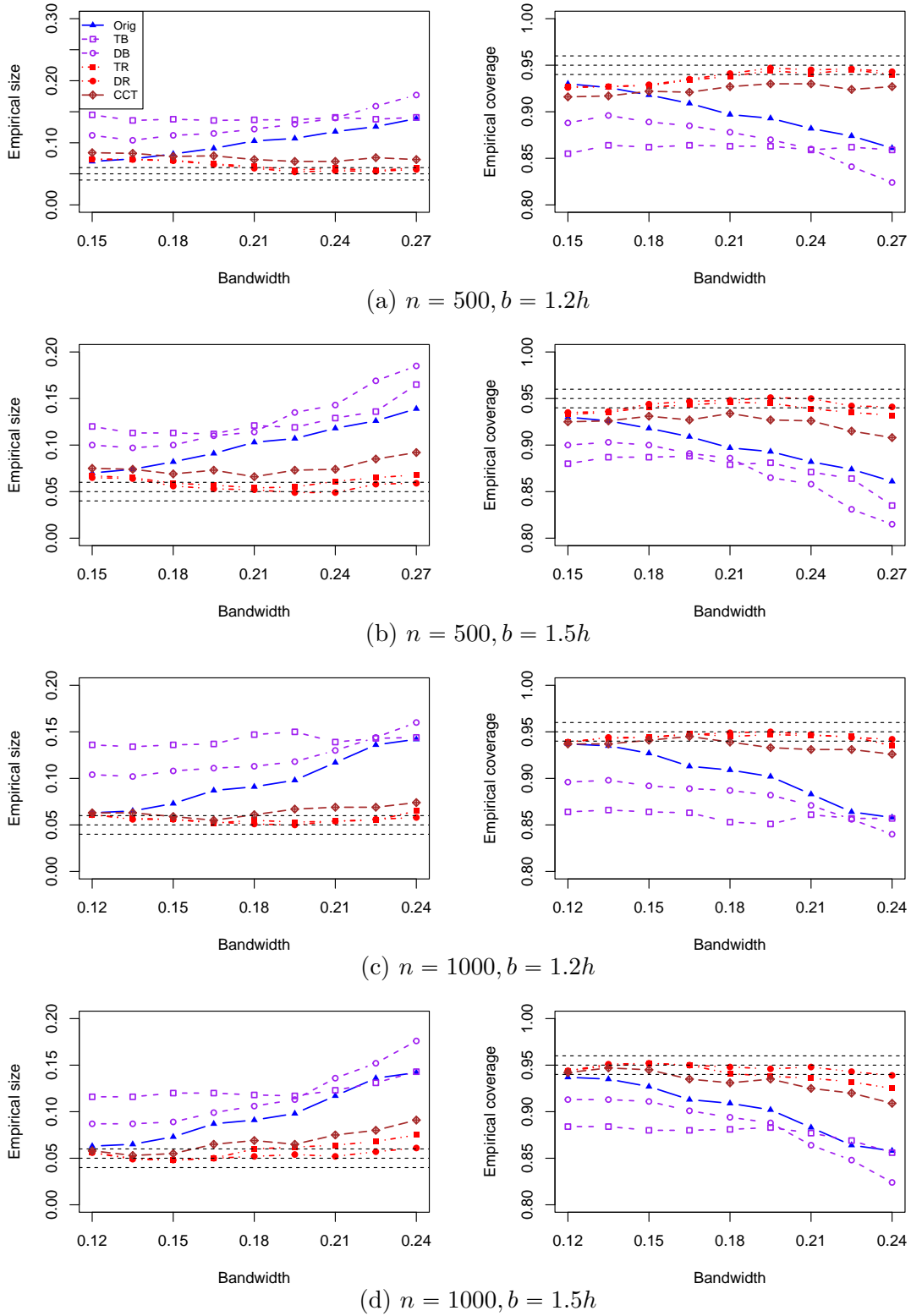


Figure 2: Plots of empirical sizes and coverages as functions of bandwidth over 1000 simulation runs for Model 3.

Table 2: Average interval lengths and empirical coverages (in parentheses) of 95% confidence intervals over 1000 simulation runs for Model 3. The best performances, with empirical coverages close to 95% and short interval lengths, are in bold font.

$h$	$n = 500$					$n = 1000$				
	0.15	0.18	0.21	0.24	0.27	0.12	0.15	0.18	0.21	0.24
Orig	0.221 (0.930)	0.203 (0.918)	0.190 (0.897)	0.179 (0.882)	0.170 (0.861)	0.176 (0.937)	0.158 (0.927)	0.145 (0.909)	0.135 (0.883)	0.127 (0.858)
Setting: $b = 1.2h$										
TB	0.245 (0.855)	0.221 (0.862)	0.204 (0.863)	0.191 (0.859)	0.181 (0.859)	0.186 (0.864)	0.166 (0.864)	0.152 (0.853)	0.142 (0.861)	0.133 (0.857)
DB	0.216 (0.888)	0.199 (0.889)	0.185 (0.878)	0.174 (0.860)	0.165 (0.824)	0.174 (0.896)	0.156 (0.892)	0.143 (0.887)	0.133 (0.871)	0.125 (0.840)
TR	0.325 (0.927)	0.293 (0.928)	0.267 (0.938)	0.249 (0.941)	<b>0.234</b> <b>(0.940)</b>	0.245 (0.939)	0.218 (0.944)	0.199 (0.945)	<b>0.185</b> <b>(0.946)</b>	0.174 (0.935)
DR	0.356 (0.926)	0.297 (0.929)	0.271 (0.941)	0.251 (0.945)	<b>0.237</b> <b>(0.943)</b>	0.250 (0.939)	0.221 (0.944)	0.201 (0.949)	0.187 (0.947)	<b>0.175</b> <b>(0.942)</b>
CCT	0.290 (0.916)	0.265 (0.922)	0.246 (0.927)	0.231 (0.930)	0.219 (0.927)	0.231 (0.937)	0.207 (0.941)	<b>0.190</b> <b>(0.939)</b>	0.176 (0.931)	0.165 (0.926)
Setting: $b = 1.5h$										
TB	0.234 (0.880)	0.213 (0.887)	0.198 (0.879)	0.186 (0.871)	0.175 (0.835)	0.182 (0.884)	0.163 (0.880)	0.150 (0.881)	0.139 (0.877)	0.130 (0.856)
DB	0.216 (0.900)	0.199 (0.900)	0.186 (0.886)	0.175 (0.858)	0.166 (0.815)	0.174 (0.913)	0.156 (0.911)	0.143 (0.894)	0.133 (0.864)	0.125 (0.824)
TR	0.299 (0.933)	0.267 (0.941)	0.246 (0.946)	<b>0.230</b> <b>(0.939)</b>	0.217 (0.932)	0.225 (0.944)	0.201 (0.952)	<b>0.184</b> <b>(0.941)</b>	0.171 (0.936)	0.160 (0.925)
DR	0.326 (0.935)	0.286 (0.944)	0.261 (0.948)	0.242 (0.950)	<b>0.228</b> <b>(0.941)</b>	0.239 (0.944)	0.212 (0.952)	0.193 (0.948)	0.179 (0.948)	<b>0.168</b> <b>(0.939)</b>
CCT	0.266 (0.925)	0.244 (0.931)	<b>0.227</b> <b>(0.934)</b>	0.213 (0.926)	0.202 (0.908)	0.212 (0.942)	<b>0.191</b> <b>(0.945)</b>	0.174 (0.931)	0.162 (0.925)	0.152 (0.909)

## 6.1 Brazilian mayoral elections

The first dataset, analyzed in [Klašnja and Titunik \(2017\)](#), contains municipal mayoral election vote shares for political parties in Brazil during the period 1996 to 2012. We aim to investigate the impact of a party’s victory in an election on its likelihood of winning the subsequent election within the same municipality. For a given party, the vote margin is defined as the difference between the party’s vote share and that of its strongest opponent in the same election. Then, the forcing variable  $X_i$  represents the vote margin at the  $t$ -th election, and the outcome variable  $Y_i$  denotes the vote margin in the subsequent  $(t + 1)$ -th election. To clarify, we only consider municipalities where the incumbent party competes for reelection at  $t + 1$ . The final dataset includes  $n = 5460$  municipalities, divided into a treatment group

Table 3: Comparison of average and standard deviation (in parentheses) of bandwidths  $h$  and  $b$ , empirical sizes, empirical coverages and average interval lengths over 10000 simulation runs for Model 3. The best performances, with empirical sizes close to 5% and empirical coverages close to 95%, are in bold font.

Method	$n = 500$					$n = 1000$				
	$h$	$b$	Size	Coverage	Length	$h$	$b$	Size	Coverage	Length
Orig	0.213 (0.041)	-	0.112	0.888	0.191	0.207 (0.04)	-	0.146	0.854	0.137
	$(h, b) = (\hat{h}_{\text{opt}}, \hat{b}_{\text{opt}})$									
TB			0.136	0.864	0.196			0.158	0.842	0.139
DB			0.141	0.859	0.187			0.172	0.828	0.134
TR	0.213 (0.041)	0.345 (0.061)	0.072	0.929	0.241	0.207 (0.040)	0.337 (0.057)	0.089	0.912	0.166
DR			<b>0.062</b>	<b>0.938</b>	0.259			<b>0.074</b>	<b>0.926</b>	0.176
CCT			0.085	0.915	0.223			0.102	0.898	0.159
	$(h, b) = (\hat{h}_{\text{opt}}, 1.2\hat{h}_{\text{opt}})$									
TB			0.143	0.857	0.205			0.156	0.844	0.142
DB			0.144	0.856	0.186			0.172	0.828	0.134
TR	0.213 (0.041)	0.255 (0.049)	<b>0.056</b>	<b>0.944</b>	0.277	0.207 (0.040)	0.248 (0.048)	<b>0.062</b>	<b>0.938</b>	0.187
DR			<b>0.054</b>	<b>0.946</b>	0.285			<b>0.060</b>	<b>0.940</b>	0.189
CCT			0.065	0.935	0.250			0.073	0.927	0.178
	$(h, b) = (\hat{h}_{\text{opt}}, 1.5\hat{h}_{\text{opt}})$									
TB			0.142	0.859	0.198			0.160	0.840	0.140
DB			0.144	0.856	0.187			0.174	0.826	0.134
TR	0.213 (0.041)	0.319 (0.061)	0.069	0.931	0.251	0.207 (0.040)	0.310 (0.059)	0.084	0.916	0.172
DR			<b>0.059</b>	<b>0.941</b>	0.271			<b>0.071</b>	<b>0.929</b>	0.181
CCT			0.081	0.919	0.229			0.096	0.904	0.164

and a control group. The treatment group consists of 3242 municipalities where the party won the  $t$ -election ( $X_i \geq 0$ ), while the control group includes 2218 municipalities where the party lost at  $t$  ( $X_i < 0$ ). We thus focus on testing whether  $\tau_S = 0$  at the cutoff point  $x = 0$ , which serves as the threshold between electoral loss and victory. For a detailed falsification analysis validating the RD design, see Cattaneo et al. (2020).

Table 4 presents  $p$ -values and confidence intervals at 95% confidence level for the competing methods, together with the selected values of  $\hat{h}_{\text{opt}}$  and  $\hat{b}_{\text{opt}}$ . Several patterns are observable. First, all methods suggest a statistically significant and negative effect with  $p$ -values close to 0. This agrees with Klašnja and Titiunik (2017), which concluded that becoming the incumbent party can lead to electoral losses in subsequent elections. Second, the three robust methods (TR, DR and CCT) produce wider confidence intervals, reflecting their

Table 4: Effect of winning at  $t$  on vote margin at  $t + 1$  for the incumbent party in Brazil.

Method	$p$ -value	95% CI	Method	$p$ -value	95% CI	$\hat{h}_{\text{opt}}$	$\hat{b}_{\text{opt}}$
Orig	0.000	[-6.586, -3.139]	CCT	0.000	[-10.271, -2.987]	15.287	27.523
TB	0.000	[-6.586, -3.442]	TR	0.001	[-10.278, -2.936]		
DB	0.000	[-6.586, -3.411]	DR	0.001	[-10.272, -2.672]		

improved ability to account for bias and variability in the bias estimation. Specifically, TR yields a confidence interval of  $[-10.278, -2.936]$ , while DR returns  $[-10.272, -2.672]$ . The CCT method provides a comparable confidence interval  $[-10.271, -2.987]$ . Third, among the robust methods, CCT delivers a symmetric confidence interval centered at  $\hat{\tau}_S$  due to its construction, whereas both TR and DR produce asymmetric and fully data-adaptive confidence intervals. Notably, DR results in a slightly wider interval compared to CCT and TR, which may indicate improved empirical coverage, as evidenced by Table 3 in Section 5.2.

## 6.2 Turkey’s female educational attainment

Our second dataset combines municipal mayoral election data from Turkey’s 1994 elections with educational attainment data from the 2000 Turkish Population Census, as analyzed in Meyersson (2014). The goal is to examine the effect of Islamic political representation in the 1994 municipal elections on high school attainment for women whose education could have been influenced between 1994 and 2000. The matched dataset includes  $n = 2629$  municipalities. The forcing variable  $X_i$  is the vote margin, defined as the vote percentage of the Islamic party minus that of its strongest secular opponent. Mayoral elections were determined by plurality, thus the municipalities with  $X_i \geq 0$  elected an Islamic mayor (treatment group), while those with  $X_i < 0$  elected a secular mayor (control group). The outcome variable  $Y_i$  measures the educational attainment of women who were potentially in high school during the study period, calculated as the percentage of women aged 15 to 20 in 2000 who had completed high school by that year. For further details and validity checks on this RD design, see Meyersson (2014).

Table 5: Effect of Islamic rule on female high school educational attainment in Turkey.

Method	$p$ -value	95% CI	Method	$p$ -value	95% CI	$\hat{h}_{\text{opt}}$	$\hat{b}_{\text{opt}}$
Orig	0.029	[0.310, 5.860]	CCT	0.074	[-0.284, 6.255]	17.491	29.124
TB	0.031	[0.276, 5.828]	TR	0.066	[-0.197, 6.344]		
DB	0.028	[0.323, 5.860]	DR	0.083	[-0.369, 6.362]		

Table 5 reports the  $p$ -values and 95% confidence intervals. While all methods suggest positive effects, the levels of significance vary. The Orig, TB and DB methods produce confidence intervals that exclude zero and yield  $p$ -values below 0.05. In contrast, the three robust methods provide intervals that include zero and are associated with  $p$ -values above 0.05, offering a more cautious and potentially more reliable interpretation of the effect of Islamic rule. Interestingly, DR again delivers a slightly wider confidence interval and a more conservative  $p$  value than TR and CCT, suggesting a higher degree of uncertainty in evaluating the influence of Islamic rule on female high school attainment.

## 7 Discussion

Our paper introduces a novel EL-based strategy for nonparametric regression and RDD inference. The key innovation lies in the development of fully data-adaptive robust weights that simultaneously correct for bias and account for its variability, thereby enabling an automatic and valid EL-based inference procedure that retains the Wilks-type chi-squared limiting distribution while exhibiting strong robustness properties. Looking ahead, several important directions remain to be explored. First, it is possible to develop Bartlett-type corrections or bootstrap adjustments within our framework as potential second-order refinements, building on techniques similar to those in [Chen and Qin \(2000\)](#) and [Otsu et al. \(2015\)](#), which typically involves substantial technical and computational complexities. Another important and related topic is bandwidth selection. In our numerical studies, we adopted the MSE-optimal bandwidth selection method in the R package `rdrobust`, which is convenient



and user-friendly. For inference purposes, however, it is of greater interest to study coverage-optimal bandwidth selection under the proposed robust EL framework. Ideally, this would be achieved without requiring additional variance estimation, potentially through higher-order asymptotic analysis and Edgeworth expansions to better characterize the coverage properties of our proposed confidence intervals. The third interesting direction is to extend the proposed approach to nonparametric quantile regression and quantile RDD; see, e.g., [Qu and Yoon \(2019\)](#) and [Xu \(2020\)](#). A key challenge in this context is how to conduct uniform inference across various quantile levels within our proposed robust EL framework. These topics fall beyond the scope of the current paper and will be pursued elsewhere.

## References

- Armstrong, T. B. and Kolesár, M. (2018). Optimal inference in a class of regression models, *Econometrica* **86**: 655–683.
- Bravo, F., Escanciano, J. C. and Van Keilegom, I. (2020). Two-step semiparametric empirical likelihood inference, *The Annals of Statistics* **48**: 1–26.
- Calonico, S., Cattaneo, M. D. and Farrell, M. H. (2018). On the effect of bias estimation on coverage accuracy in nonparametric inference, *Journal of the American Statistical Association* **113**: 767–779.
- Calonico, S., Cattaneo, M. D. and Titiunik, R. (2014). Robust nonparametric confidence intervals for regression-discontinuity designs, *Econometrica* **82**: 2295–2326.
- Cattaneo, M. D., Idrobo, N. and Titiunik, R. (2019). *A practical introduction to regression discontinuity designs: Foundations*, Cambridge University Press.
- Cattaneo, M. D., Idrobo, N. and Titiunik, R. (2024). *A practical introduction to regression discontinuity designs: Extensions*, Cambridge University Press.
- Cattaneo, M. D., Titiunik, R. and Vazquez-Bare, G. (2020). The regression discontinuity design, in L. Curini and R. J. Franzese (eds), *Handbook of Research Methods in Political Science and International Relations*, Sage Publications, London, UK, chapter 44, pp. 835–857.
- Chen, S. X. and Qin, Y. S. (2000). Empirical likelihood confidence intervals for local linear smoothers, *Biometrika* **87**: 946–953.

- Chen, S. X. and Van Keilegom, I. (2009). A review on empirical likelihood methods for regression, *Test* **18**: 415–447.
- Chiang, H. D., Hsu, Y.-C. and Sasaki, Y. (2019). Robust uniform inference for quantile treatment effects in regression discontinuity designs, *Journal of Econometrics* **211**: 589–618.
- Dong, Y., Lee, Y.-Y. and Gou, M. (2023). Regression discontinuity designs with a continuous treatment, *Journal of the American Statistical Association* **118**: 208–221.
- Fan, J., Farmen, M. and Gijbels, I. (1998). Local maximum likelihood estimation and inference, *Journal of the Royal Statistical Society. Series B. Statistical Methodology* **60**: 591–608.
- Fan, J. and Gijbels, I. (1996). *Local polynomial modelling and its applications*, Chapman & Hall, London.
- Fan, J. and Zhang, W. (1999). Statistical estimation in varying coefficient models, *The Annals of Statistics* **27**: 1491–1518.
- Hahn, J., Todd, P. and Van der Klaaw, W. (2001). Identification and estimation of treatment effects with a regression-discontinuity design, *Econometrica* **69**: 201–209.
- Imbens, G. and Kalyanaraman, K. (2012). Optimal bandwidth choice for the regression discontinuity estimator, *Review of Economic Studies* **79**: 933–959.
- Kitamura, Y., Tripathi, G. and Ahn, H. (2004). Empirical likelihood-based inference in conditional moment restriction models, *Econometrica* **72**: 1667–1714.
- Klašnja, M. and Titiumik, R. (2017). The incumbency curse: Weak parties, term limits, and unfulfilled accountability, *American Political Science Review* **111**: 129–148.
- Lee, D. S. (2008). Randomized experiments from non-random selection in U.S. House elections, *Journal of Econometrics* **142**: 675–697.
- Ma, J. and Yu, Z. (2020). Empirical likelihood covariate adjustment for regression discontinuity designs, *arXiv:2008.09263* .
- Matsushita, Y. and Otsu, T. (2021). Jackknife empirical likelihood: small bandwidth, sparse network and high-dimensional asymptotics, *Biometrika* **108**: 661–674.
- Meyersson, E. (2014). Islamic rule and the empowerment of the poor and pious, *Econometrica* **82**: 229–269.

- Otsu, T. (2012). Empirical likelihood for nonparametric additive models, *Journal of the Japan Statistical Society* **41**: 159–186.
- Otsu, T., Xu, K.-L. and Matsushita, Y. (2015). Empirical likelihood for regression discontinuity design, *Journal of Econometrics* **186**: 94–112.
- Owen, A. B. (1988). Empirical likelihood ratio confidence intervals for a single functional, *Biometrika* **75**: 237–249.
- Owen, A. B. (1990). Empirical likelihood ratio confidence regions, *The Annals of Statistics* **18**: 90–120.
- Owen, A. B. (2001). *Empirical likelihood*, Chapman and Hall/CRC.
- Qu, Z. and Yoon, J. (2019). Uniform inference on quantile effects under sharp regression discontinuity designs, *Journal of Business & Economic Statistics* **37**: 625–647.
- Wang, H., Zhong, P.-S., Cui, Y. and Li, Y. (2018). Unified empirical likelihood ratio tests for functional concurrent linear models and the phase transition from sparse to dense functional data, *Journal of the Royal Statistical Society Series B: Statistical Methodology* **80**: 343–364.
- Xu, K.-L. (2013). Nonparametric inference for conditional quantiles of time series, *Economic Theory* **29**: 673–698.
- Xu, K.-L. (2020). Inference of local regression in the presence of nuisance parameters, *Journal of Econometrics* **218**: 532–560.
- Xue, L. (2023). Two-stage estimation and bias-corrected empirical likelihood in a partially linear single-index varying-coefficient model, *Journal of the Royal Statistical Society Series B: Statistical Methodology* **85**: 1299–1325.
- Xue, L. and Zhu, L. (2007a). Empirical likelihood for a varying coefficient model with longitudinal data, *Journal of the American Statistical Association* **102**: 642–654.
- Xue, L. and Zhu, L. (2007b). Empirical likelihood semiparametric regression analysis for longitudinal data, *Biometrika* **94**: 921–937.
- Yu, W. and Bondell, H. D. (2024). Variational Bayes for fast and accurate empirical likelihood inference, *Journal of the American Statistical Association* **119**: 1089–1101.

# Supplementary Material to “On Robust Empirical Likelihood for Nonparametric Regression with Application to Regression Discontinuity Designs”

Qin Fang, Shaojun Guo, Yang Hong and Xinghao Qiao

This supplementary material contains proofs of main theoretical results in Section [A](#), and additional empirical results in Section [B](#).

## A Proofs of main theoretical results

### A.1 Proof of Theorem [1](#)

We focus on proving part (b) of Theorem [1](#). Part (a) then follows by setting  $\kappa = 0$ .

#### A.1.1 Asymptotic distribution of $l_{\text{TB}}\{m(x)\}$

Recall that  $Z_i(x) = W_{i,h}(x)\{Y_i - 2^{-1}\widehat{m}_{2,b}^{(2)}(x)(X_i - x)^2 - m(x)\}$ , and

$$U_1(x) = \frac{1}{n} \sum_{i=1}^n Z_i(x), \quad U_2(x) = \frac{1}{n} \sum_{i=1}^n \{Z_i(x)\}^2.$$

Using the Lagrange multiplier method, we have that

$$l_{\text{TB}}\{m(x)\} = 2 \sum_{i=1}^n \log \{1 + \lambda Z_i(x)\},$$

where  $\lambda$  satisfies the equation

$$\sum_{i=1}^n \frac{Z_i(x)}{1 + \lambda Z_i(x)} = 0. \tag{S.1}$$

Analogous to the proofs in [Owen \(2001\)](#), we structure the proof in four steps to establish the asymptotic distribution of  $l_{\text{TB}}\{m(x)\}$ . Firstly, we demonstrate the asymptotic distribution of  $U_1(x)$ , i.e.,

$$\sqrt{nh}U_1(x) \xrightarrow{\mathcal{D}} N(0, \sigma_{1,\kappa}^2(x)), \tag{S.2}$$

and

$$hU_2(x) = \sigma_0^2(x)\{1 + o_P(1)\}, \quad (\text{S.3})$$

where the formulas for  $\sigma_{1,\kappa}^2(x)$  and  $\sigma_0^2(x)$  will be provided later. Notably, if  $\kappa > 0$ , then  $\sigma_{1,\kappa}^2(x) \neq \sigma_0^2(x)$ ; otherwise,  $\sigma_{1,0}^2(x) = \sigma_0^2(x)$ . Next, we show that

$$\max_{1 \leq i \leq n} |Z_i(x)| = o_P(n^{1/2}h^{-1/2}), \quad \lambda = O_P(n^{-1/2}h^{1/2}), \quad (\text{S.4})$$

and further establish that

$$\lambda = U_2^{-1}(x)U_1(x) + o_P(n^{-1/2}h^{1/2}). \quad (\text{S.5})$$

Combining (S.2)–(S.5) and noting that  $|\lambda| \max_{i \leq n} |Z_i(x)| = o_P(1)$ , by applying Taylor's expansion, i.e.,  $\log(1+x) = x - 2^{-1}x^2 + o(x^2)$ , we can write  $l_{\text{TB}}\{m(x)\}$  as

$$\begin{aligned} l_{\text{TB}}\{m(x)\} &= 2 \sum_{i=1}^n \log \{1 + \lambda Z_i(x)\} \\ &= 2\lambda \sum_{i=1}^n Z_i(x) - \lambda^2 \sum_{i=1}^n Z_i^2(x) \{1 + o_P(1)\} \\ &= \frac{\sigma_{1,\kappa}^2(x)}{\sigma_0^2(x)} \left\{ \frac{\sqrt{nh}U_1(x)}{\sigma_{1,\kappa}(x)} \right\}^2 \{1 + o_P(1)\}, \end{aligned}$$

implying that  $l_{\text{TB}}\{m(x)\} \xrightarrow{D} \gamma_{1,\kappa} \chi_1^2$ , where  $\gamma_{1,\kappa} = \sigma_{1,\kappa}^2(x)/\sigma_0^2(x)$ .

We now provide the proofs for equations (S.2)–(S.5). To begin, we introduce some notation. Define  $\mathbf{S}$  as the matrix  $(\mu_{j+k-2})_{1 \leq j, k \leq 3}$ , and let  $\mu_j = \int_{-1}^1 u^j K(u) du$ ,  $\nu_j = \int_{-1}^1 u^j K(u)^2 du$  for  $j = 0, \dots, 4$ . Note that, in particular,  $\mu_0 = 1$  and  $\mu_1 = \mu_3 = 0$ . Additionally, we define  $w_{i,h}(x) = \mu_2 K_h(X_i - x)$  for  $i = 1, \dots, n$ .

We first demonstrate that the asymptotic distribution of  $U_1(x)$ . Recall that

$$\hat{m}_{2,b}^{(2)}(x) = \frac{2}{nb^2} \sum_{i=1}^n W_{i,2,2,b}(x) Y_i,$$

where  $W_{i,2,2,b}(x) = \mathbf{e}_3^\top \mathbf{S}_{2,b}^{-1} \{1, (X_i - x)/b, (X_i - x)^2/b^2\}^\top K_b(X_i - x)$ . Given that  $m(x)$  is continuously differentiable up to the third order in the neighborhood of  $x$ , it follows from Section 3.2.2 in [Fan and Gijbels \(1996\)](#) that

$$\hat{m}_{2,b}^{(2)}(x) - m^{(2)}(x) = O_P(b) + \frac{2}{nb^2 f(x)} \sum_{i=1}^n \tilde{w}_{i,b}(x) \varepsilon_i \{1 + o_P(1)\},$$

where  $\tilde{w}_{i,b}(x) = \mathbf{e}_3^\top \mathbf{S}^{-1} \{1, (X_i - x)/b, (X_i - x)^2/b^2\}^\top K_b(X_i - x)$ . This further implies that  $\hat{m}_{2,b}^{(2)}(x) - m^{(2)}(x) = O_P\{b + (nb^5)^{-1/2}\}$ .

Note that  $\sum_{i=1}^n (X_i - x)W_{i,h}(x) = 0$ ,  $W_{i,h}(x) = w_{i,h}(x)f(x)\{1 + o_P(1)\}$ , and

$$\sum_{i=1}^n (X_i - x)^2 W_{i,h}(x) = nh^2 f^2(x) \mu_2^2 \{1 + o_P(1)\}.$$

The term  $U_1(x)$  can be reformulated as

$$\begin{aligned} U_1(x) &= \frac{1}{n} \sum_{i=1}^n W_{i,h}(x) \{r(X_i) + \varepsilon_i\} - \frac{1}{2n} \sum_{i=1}^n W_{i,h}(x) (X_i - x)^2 \{\hat{m}_{2,b}^{(2)}(x) - m^{(2)}(x)\} \\ &= O_P(h^3 + h^2b) + \frac{1}{n} \sum_{i=1}^n W_{i,h}(x) \varepsilon_i - \frac{h^2 \mu_2^2 f(x)}{nb^2} \sum_{i=1}^n \tilde{w}_{i,b}(x) \varepsilon_i \{1 + o_P(1)\} \\ &= O_P(h^3 + h^2b) + \frac{f(x)}{n} \sum_{i=1}^n \{w_{i,h}(x) - \kappa^2 \mu_2^2 \tilde{w}_{i,b}(x)\} \varepsilon_i \{1 + o_P(1)\}. \end{aligned}$$

Given that  $\sqrt{nh}(h^3 + h^2b) \rightarrow 0$  since  $nh^5b^2 \rightarrow 0$  and  $h/b \rightarrow \kappa \in [0, 1]$ , by the classic central limit theorem, we obtain [\(S.2\)](#), where

$$\sigma_{1,\kappa}^2(x) = \lim_{h/b \rightarrow \kappa, b \rightarrow 0} hE\{w_{i,h}(x) - \kappa^2 \mu_2^2 \tilde{w}_{i,b}(x)\}^2 \sigma^2(x) f^2(x),$$

and this limit exists.

We write the term  $U_2(x)$  as

$$U_2(x) = \frac{1}{n} \sum_{i=1}^n \{W_{i,h}(x)\}^2 \{\varepsilon_i + o_P(1)\}^2 = \frac{1}{n} \sum_{i=1}^n w_{i,h}^2(x) \varepsilon_i^2 f^2(x) (1 + o_P(1)).$$

This implies  $hU_2(x) = \sigma_0^2(x)\{1 + o_P(1)\}$ , where  $\sigma_0^2(x) = \mu_2^2\nu_0\sigma^2(x)f^3(x)$ , which is equal to  $\sigma_{1,0}^2(x)$ , and hence (S.3) follows.

Now we turn to show that  $\max_{1 \leq i \leq n} |Z_i(x)| = o_P(n^{1/2}h^{-1/2})$ . Observe that  $|S_{2,h}(x)| + |S_{1,h}(x)| = O_P(1)$ , we have

$$\begin{aligned} \max_{1 \leq i \leq n} |Z_i(x)| &\leq \max_{1 \leq i \leq n} \{K_h(X_i - x)\{|\varepsilon_i| + o(1)\}\} \cdot O_P(1) \\ &\quad + \max_{1 \leq i \leq n} \{K_h(X_i - x)\} O_P\{h^2b + h^2(nb^5)^{-1/2}\} \\ &\leq \max_{1 \leq i \leq n} \{K_h(X_i - x)\{|\varepsilon_i| + O(1)\}\} \cdot O_P(1). \end{aligned}$$

Since  $E\{K_h^4(X_i - x)\varepsilon_i^4\} = O(h^{-3})$ , it follows from Markov inequality that

$$\max_{1 \leq i \leq n} |K_h(X_i - x)\varepsilon_i| = o_P(n^{1/2}h^{-1/2}).$$

which further implies that  $\max_{1 \leq i \leq n} |Z_i(x)| = o_P(n^{1/2}h^{-1/2})$ .

Next, we show that  $\lambda = O_P(n^{-1/2}h^{1/2})$ . From Equation (S.1), we have

$$\sum_{i=1}^n Z_i(x) = \sum_{i=1}^n \frac{\lambda Z_i^2(x)}{1 + \lambda Z_i(x)}.$$

Since each  $p_i \geq 0$ ,  $1 + \lambda Z_i(x) > 0$ , and therefore,

$$\frac{1}{n} \sum_{i=1}^n \frac{Z_i^2(x)}{1 + \lambda Z_i(x)} \geq \frac{U_2(x)}{1 + |\lambda| \max_{i \leq n} |Z_i(x)|}.$$

This inequality implies that

$$|\lambda|U_2(x) \leq \left(1 + |\lambda| \max_{i \leq n} |Z_i(x)|\right) \left|\frac{1}{n} \sum_{i=1}^n Z_i(x)\right|.$$

Thus we conclude that

$$\begin{aligned} |\lambda|\sigma_2^2(x)\{1 + o_P(1)\} &\leq h \cdot O_P\{(nh)^{-1/2}\} + |\lambda| \cdot h \cdot o_P(n^{1/2}h^{-1/2}) \cdot O_P\{(nh)^{-1/2}\} \\ &\leq h \cdot O_P\{(nh)^{-1/2}\} + |\lambda| \cdot o_P(1), \end{aligned}$$

which in turn implies that  $|\lambda| = O_P(n^{-1/2}h^{1/2})$ .

Finally, we show that  $\lambda = U_2^{-1}U_1(x) + o_P(n^{-1/2}h^{1/2})$ . First, we observe that

$$0 = \sum_{i=1}^n \frac{Z_i(x)}{1 + \lambda Z_i(x)} = \sum_{i=1}^n Z_i(x) - \lambda \sum_{i=1}^n Z_i^2(x) + \sum_{i=1}^n \frac{\lambda^2 Z_i^3(x)}{1 + \lambda Z_i(x)}.$$

Note that  $|\lambda| \max_{i \leq n} |Z_i(x)| = o_P(1)$ . Hence it follows that

$$\left| \sum_{i=1}^n \frac{\lambda^2 Z_i^3(x)}{1 + \lambda Z_i(x)} \right| \leq o_P(|\lambda|) \cdot \sum_{i=1}^n \frac{Z_i^2(x)}{1 - o_P(1)} \leq o_P(|\lambda|) \sum_{i=1}^n Z_i^2(x) \{1 + o_P(1)\}.$$

As a result, we obtain that

$$\lambda = \left\{ \sum_{i=1}^n Z_i^2(x) \right\}^{-1} \sum_{i=1}^n Z_i(x) + o_P(|\lambda|) = U_2^{-1}U_1(x) + o_P(n^{-1/2}h^{1/2}).$$

The proof for  $l_{\text{TB}}\{m(x)\}$  is complete.

### A.1.2 Asymptotic distribution of $l_{\text{DB}}\{m(x)\}$

Define  $\tilde{Z}_i(x) = W_{i,h}(x)\{Y_i - m(x) - (\hat{m}_{2,b}(X_i) - \hat{m}_{2,b}(x))\}$ , and let

$$\tilde{U}_1(x) = \frac{1}{n} \sum_{i=1}^n \tilde{Z}_i(x), \quad \tilde{U}_2(x) = \frac{1}{n} \sum_{i=1}^n \{\tilde{Z}_i(x)\}^2.$$

Through the Lagrange multiplier approach, we have that

$$l_{\text{DB}}\{m(x)\} = 2 \sum_{i=1}^n \log \{1 + \lambda \tilde{Z}_i(x)\},$$



where  $\lambda$  satisfies the equation

$$\sum_{i=1}^n \frac{\tilde{Z}_i(x)}{1 + \lambda \tilde{Z}_i(x)} = 0.$$

Similar to the proof techniques outlined in Section A.1.1, it can be straightforwardly shown that

$$h\tilde{U}_2(x) = \sigma_0^2(x)\{1 + o_P(1)\}, \quad \max_{1 \leq i \leq n} |\tilde{Z}_i(x)| = o_P(n^{1/2}h^{-1/2}), \quad \lambda = O_P(n^{-1/2}h^{1/2}),$$

and furthermore, it can be established that  $\lambda = \tilde{U}_2^{-1}(x)\tilde{U}_1(x) + o_P(n^{-1/2}h^{1/2})$ . These derivations are therefore omitted here for brevity. If we establish that

$$\sqrt{nh}\tilde{U}_1(x) \xrightarrow{\mathcal{D}} N(0, \sigma_{2,\kappa}^2(x)), \tag{S.6}$$

then we can write  $l_{\text{DB}}\{m(x)\}$  as follows:

$$\begin{aligned} l_{\text{DB}}\{m(x)\} &= 2\lambda \sum_{i=1}^n \tilde{Z}_i(x) - \lambda^2 \sum_{i=1}^n \{\tilde{Z}_i(x)\}^2 \{1 + o_P(1)\} \\ &= \frac{\sigma_{2,\kappa}^2(x)}{\sigma_0^2(x)} \left\{ \frac{\sqrt{nh}\tilde{U}_1(x)}{\sigma_{2,\kappa}(x)} \right\}^2 \{1 + o_P(1)\}, \end{aligned}$$

implying that  $l_{\text{DB}}\{m(x)\} \xrightarrow{\mathcal{D}} \gamma_{2,\kappa}\chi_1^2$ , where  $\gamma_{2,\kappa} = \sigma_{2,\kappa}^2(x)/\sigma_0^2(x)$ . Therefore, in the following discussion, we will focus on deriving the asymptotic distribution of  $\tilde{U}_1(x)$ , which corresponds to (S.6).

First, it follows from Lemma 1 of Fan and Zhang (1999) that

$$\hat{m}_{2,b}(x) - m(x) = \frac{1}{nf(x)} \sum_{i=1}^n \check{w}_{i,b}(x)\varepsilon_i + O_P\left(b^3 + \frac{b^2 \log^{1/2} n}{n^{1/2}b^{1/2}} + \frac{\log n}{nb}\right),$$

holds uniformly over  $x \in [0, 1]$ , where  $\check{w}_{i,b}(x) = \mathbf{e}_1^\top \mathbf{S}^{-1} \{1, (X_i - x)/b, (X_i - x)^2/b^2\}^\top K_b(X_i - x)$ .

Given that  $b^2 \log n \rightarrow 0$  and  $nh^3b^4 \rightarrow 0$ , for each  $X_i$  and  $x$ ,

$$\hat{m}_{2,b}(X_i) - \hat{m}_{2,b}(x) = m(X_i) - m(x) + \frac{1}{nf(x)} \sum_{k=1}^n \{\check{w}_{k,b}(X_i) - \check{w}_{k,b}(x)\} \varepsilon_k + o_P\{(nh)^{-1/2}\},$$

The term  $\tilde{U}_1(x)$  can then be written as follows:

$$\tilde{U}_1(x) = \frac{f(x)}{n} \sum_{i=1}^n w_{i,h}(x) \varepsilon_i - \frac{1}{n} \sum_{i=1}^n \frac{1}{n} \sum_{k=1}^n w_{k,h}(x) \{\check{w}_{i,b}(X_k) - \check{w}_{i,b}(x)\} \varepsilon_i + o_P\{(nh)^{-1/2}\}.$$

Denote an equivalent kernel  $\check{K}(t)$  by

$$\check{K}(t) = \mathbf{e}_1^\top \mathbf{S}^{-1} \int_{-1}^1 \{1, t - \kappa u, (t - \kappa u)^2\}^\top K(u) K(t - \kappa u) du,$$

and  $\check{K}_{i,b}(x) = \check{K}\{(X_i - x)/b\}/b$ , for  $i = 1, \dots, n$ . We can show that for each  $X_i$  and  $x$ ,

$$\frac{1}{n} \sum_{k=1}^n E_{X_k} \{w_{k,h}(x) \check{w}_{i,b}(X_k)\} = \mu_2 \check{K}_{i,b}(x) f(x) \{1 + o(1)\},$$

Moreover, for each  $X_i$  and  $x$ , the corresponding variance is

$$\frac{1}{n^2} \sum_{j=1}^n \text{Var}_{X_j} \{w_{j,h}(x) \check{w}_{i,b}(X_k)\} = O\{(nhb^2)^{-1}\} = o(h^{-1}).$$

since  $nb^2 \rightarrow \infty$  as  $n \rightarrow \infty$ . Note that  $n^{-1} \sum_{k=1}^n w_{k,h}(x) = \mu_2 f(x) \{1 + o_P(1)\}$ . Therefore,

$$\frac{1}{n} \sum_{k=1}^n w_{k,h}(x) \{\check{w}_{i,b}(X_k) - \check{w}_{i,b}(x)\} = \mu_2 f(x) \{\check{K}_{i,b}(x) - \check{w}_{i,b}(x)\} \{1 + o_P(1)\}.$$

This yields that

$$\tilde{U}_1(x) = \frac{f(x)}{n} \sum_{i=1}^n \{w_{i,h}(x) - \mu_2 \check{K}_{i,b}(x) + \mu_2 \check{w}_{i,b}(x)\} \varepsilon_i + o_P\{(nh)^{-1/2}\}.$$

Then, by the classic central limit theorem, we obtain that

$$\sqrt{nh}\tilde{U}_1(x) \xrightarrow{\mathcal{D}} N(0, \sigma_{2,\kappa}^2(x)),$$

where  $\sigma_{2,\kappa}^2(x) = \lim_{h/b \rightarrow \kappa, b \rightarrow 0} hE\{w_{i,h}(x) - \mu_2\check{K}_{i,b}(x) + \mu_2\check{w}_{i,b}(x)\}^2 \sigma^2(x) f^2(x)$ , and this limit exists.

It is obvious that when  $\kappa = 0$ ,  $\sigma_{2,0}^2(x) = \sigma_0^2(x)$ .

The proof for  $l_{\text{DB}}\{m(x)\}$  is complete. □

## A.2 Proof of Theorem 2

### A.2.1 Asymptotic distribution of $l_{\text{TR}}\{m(x)\}$

Define  $Z_i^*(x) = W_{i,h,b}^*(x)\{Y_i - m(x)\}$ , and let

$$U_1^*(x) = \frac{1}{n} \sum_{i=1}^n Z_i^*(x), \quad U_2^*(x) = \frac{1}{n} \sum_{i=1}^n \{Z_i^*(x)\}^2.$$

By the Lagrange multiplier method, we have that

$$l_{\text{TR}}\{m(x)\} = 2 \sum_{i=1}^n \log \{1 + \lambda Z_i^*(x)\},$$

where  $\lambda$  is determined by the equation

$$\sum_{i=1}^n \frac{Z_i^*(x)}{1 + \lambda Z_i^*(x)} = 0.$$

Following similar proof techniques as in Section A.1.1, it can be readily shown that

$$\max_{1 \leq i \leq n} |Z_i^*(x)| = o_P(n^{1/2}h^{-1/2}), \quad \lambda = O_P(n^{-1/2}h^{1/2}),$$

Since  $U_1^\star(x)$  is identical to  $U_1(x)$  in Section A.1.1, we have  $\sqrt{nh}U_1^\star(x) \xrightarrow{\mathcal{D}} N(0, \sigma_{1,\kappa}^2(x))$ . Therefore, these derivations are omitted here. Suppose we can demonstrate that

$$hU_2^\star(x) = \sigma_{1,\kappa}^2(x)\{1 + o_P(1)\}. \quad (\text{S.7})$$

It immediately follows that  $\lambda = \{U_2^\star(x)\}^{-1}U_1^\star(x) + o_P(n^{-1/2}h^{1/2})$ . We can then write  $l_{\text{TR}}\{m(x)\}$  as follows:

$$\begin{aligned} l_{\text{TR}}\{m(x)\} &= 2\lambda \sum_{i=1}^n Z_i^\star(x) - \lambda^2 \sum_{i=1}^n \{Z_i^\star(x)\}^2 \{1 + o_P(1)\} \\ &= \left\{ \frac{\sqrt{nh}U_1^\star(x)}{\sigma_{1,\kappa}(x)} \right\}^2 \{1 + o_P(1)\} \xrightarrow{\mathcal{D}} \chi_1^2. \end{aligned}$$

We thus focus on deriving (S.7) in the remainder of the proof.

Write  $r_i(x) = m(X_i) - m(x)$ . Then

$$\begin{aligned} Z_i^\star(x) &= W_{i,h,b}^\star(x)\{Y_i - m(x)\} \\ &= W_{i,h}(x)\{r_i(x) + \varepsilon_i\} - \frac{1}{n} \sum_{k=1}^n W_{k,h}(x)(X_k - x)^2 b^{-2} W_{i,2,2,b}(x)\{r_i(x) + \varepsilon_i\} \\ &= \left\{ W_{i,h}(x)\varepsilon_i - \frac{1}{n} \sum_{k=1}^n W_{k,h}(x)(X_k - x)^2 b^{-2} W_{i,2,2,b}(x)\varepsilon_i \right\} \\ &\quad + W_{i,h}(x)r_i(x) - \frac{1}{n} \sum_{k=1}^n W_{k,h}(x)(X_k - x)^2 b^{-2} W_{i,2,2,b}(x)r_i(x) \\ &\equiv Z_{i,1}(x) + Z_{i,2}(x) + Z_{i,3}(x). \end{aligned}$$

Let  $U_{21}^\star(x) = n^{-1} \sum_{i=1}^n \{Z_{i,1}(x)\}^2$ . It is simple to show that

$$hU_{21}^\star(x) = \frac{h}{n} \sum_{i=1}^n \{w_{i,h}(x) - \kappa^2 \mu_2^2 \tilde{w}_{i,b}(x)\}^2 \varepsilon_i^2 f^2(x) \{1 + o_P(1)\} = \sigma_{1,\kappa}^2(x) \{1 + o_P(1)\}.$$

Note that  $r_i(x) = m(X_i) - m(x) = O(|X_i - x|)$  around  $x$ . We have

$$\begin{aligned} hU_{22}^*(x) &= \frac{h}{n} \sum_{i=1}^n \{Z_{i,2}(x)\}^2 = \frac{h}{n} \sum_{i=1}^n \{w_{i,h}(x)\}^2 r_i^2(X_i) f^2(x) \{1 + o_P(1)\} = O_P(h^2), \\ hU_{23}^*(x) &= \frac{h}{n} \sum_{i=1}^n \{Z_{i,3}(x)\}^2 = \frac{h}{n} \sum_{i=1}^n \kappa^4 c_1^2 \{\tilde{w}_{i,b}(x)\}^2 r_i^2(X_i) f^2(x) \{1 + o_P(1)\} = O_P(b^2). \end{aligned}$$

Therefore, by the Cauchy–Schwarz inequality, we show that

$$\begin{aligned} \frac{h}{n} \left| \sum_{i=1}^n Z_{i,1}(x) Z_{i,2}(x) \right| &\leq \{hU_{21}^*(x)\}^{1/2} \{hU_{22}^*(x)\}^{1/2} = O_P(h), \\ \frac{h}{n} \left| \sum_{i=1}^n Z_{i,1}(x) Z_{i,3}(x) \right| &\leq \{hU_{21}^*(x)\}^{1/2} \{hU_{23}^*(x)\}^{1/2} = O_P(b), \\ \frac{h}{n} \left| \sum_{i=1}^n Z_{i,2}(x) Z_{i,3}(x) \right| &\leq \{hU_{22}^*(x)\}^{1/2} \{hU_{23}^*(x)\}^{1/2} = O_P(hb), \end{aligned}$$

and hence,

$$hU_2^*(x) = \sigma_{1,\kappa}^2(x) \{1 + o_P(1)\}.$$

The proof for  $l_{\text{TR}}\{m(x)\}$  is complete.

### A.2.2 Asymptotic distribution of $l_{\text{DR}}\{m(x)\}$

Let  $Z_i^\diamond(x) = W_{i,h,b}^\diamond(x) \{Y_i - m(x)\}$ ,  $i = 1, \dots, n$  and  $U_2^\diamond(x) = n^{-1} \sum_{i=1}^n \{Z_i^\diamond(x)\}^2$ . Following similar arguments as in Section A.2.1, it suffices to show that

$$hU_2^\diamond(x) = \sigma_{2,\kappa}^2(x) \{1 + o_P(1)\}.$$

Observe that

$$\begin{aligned}
Z_i^\diamond(x) &= W_{i,h}(x)\{r_i(x) + \varepsilon_i\} - \frac{1}{n} \sum_{k=1}^n W_{k,h}(x)\{W_{i,0,2,b}(X_k) - W_{i,0,2,b}(x)\}\{r_i(x) + \varepsilon_i\} \\
&= \left[ W_{i,h}(x)\varepsilon_i - \frac{1}{n} \sum_{k=1}^n W_{k,h}(x)\{W_{i,0,2,b}(X_k) - W_{i,0,2,b}(x)\}\varepsilon_i \right] \\
&\quad + W_{i,h}(x)r_i(x) - \frac{1}{n} \sum_{k=1}^n W_{k,h}(x)\{W_{i,0,2,b}(X_k) - W_{i,0,2,b}(x)\}r_i(x) \\
&\equiv Z_{i,1}^\diamond(x) + Z_{i,2}^\diamond(x) + Z_{i,3}^\diamond(x).
\end{aligned}$$

with  $r_i(x) = m(X_i) - m(x)$ . Note that  $W_{i,h} = w_{i,h}f(x)\{1 + o_P(1)\}$ , and

$$\frac{1}{n} \sum_{k=1}^n W_{k,h}(x)\{W_{i,0,2,b}(X_k) - W_{i,0,2,b}(x)\} = \{\check{K}_{i,b}(x) - \check{w}_{i,b}(x)\}\mu_2 f(x)\{1 + o_P(1)\},$$

where  $\check{K}_{i,b}(x)$  is defined in Section A.1.2. Then,

$$\begin{aligned}
hU_{21}^\diamond(x) &= \frac{h}{n} \sum_{i=1}^n \{Z_{i,1}^\diamond(x)\}^2 \\
&= \frac{h}{n} \sum_{i=1}^n \{w_{i,h}(x) - \mu_2 \check{K}_{i,b}(x) + \mu_2 \check{w}_{i,b}(x)\}^2 \varepsilon_i^2 f^2(x)\{1 + o_P(1)\} \\
&= \sigma_{2,\kappa}^2(x)\{1 + o_P(1)\}.
\end{aligned}$$

Since  $r_i(x) = m(X_i) - m(x) = O(|X_i - x|)$  around  $x$ , we have

$$\begin{aligned}
hU_{22}^\diamond(x) &= \frac{h}{n} \sum_{i=1}^n \{Z_{i,2}^\diamond(x)\}^2 = \frac{h}{n} \sum_{i=1}^n \{w_{i,h}(x)\}^2 r_i^2(X_i) f^2(x)\{1 + o_P(1)\} = O_P(h^2), \\
hU_{23}^\diamond(x) &= \frac{h}{n} \sum_{i=1}^n \{Z_{i,3}^\diamond(x)\}^2 = \frac{h}{n} \sum_{i=1}^n \{\check{K}_{i,b}(x) - \check{w}_{i,b}(x)\}^2 r_i^2(X_i) \mu_2^2 f^2(x)\{1 + o_P(1)\} = O_P(b^2).
\end{aligned}$$

Moreover, by Cauchy–Schwartz inequality, we obtain that

$$\frac{h}{n} \sum_{i=1}^n \{Z_{i,1}^\diamond(x)Z_{i,2}^\diamond(x) + Z_{i,1}^\diamond(x)Z_{i,3}^\diamond(x) + Z_{i,2}^\diamond(x)Z_{i,3}^\diamond(x)\} = O_P(h + b).$$

Hence, it follows that

$$hU_2^\diamond(x) = \sigma_{2,\kappa}^2(x)\{1 + o_P(1)\}.$$

The proof for  $l_{\text{DR}}\{m(x)\}$  is complete.  $\square$

### A.3 Proofs of Theorems 3 and 4

We begin by introducing some notation and useful asymptotic results. Recall

$$\mathbf{Z}_i^*(\theta, a) = (W_{i,h,b}^{*+}(Y_i - \theta - a), W_{i,h,b}^{*-}(Y_i - a))^T.$$

Define  $\mathbf{W}_i = (W_{i,h,b}^{*+}, W_{i,h,b}^{*-})^T$ . Let  $\widehat{\mathbf{W}}_n = n^{-1} \sum_{i=1}^n \mathbf{W}_i$ ,  $\mathbf{U}_n = n^{-1} \sum_{i=1}^n \mathbf{Z}_i^*(\tau_S, \mu_-)$ , and

$$\widehat{\mathbf{V}}_n = \frac{1}{n} \sum_{i=1}^n \mathbf{Z}_i^*(\tau_S, \mu_-) \mathbf{Z}_i^*(\tau_S, \mu_-)^T.$$

Note that the first and second components of  $\mathbf{U}_n$  correspond to the bias-corrected local linear estimators  $\widehat{\mu}_+$  and  $\widehat{\mu}_-$ , respectively, as defined in [Calonico et al. \(2014\)](#). Let  $c_k = \int_0^1 K(u)u^k du$  for  $k = 0, 1, 2$ . By Lemma A1 and Theorem A1 in [Calonico et al. \(2014\)](#), under Conditions 3–7, it follows that

$$\sqrt{nh}\mathbf{U}_n \xrightarrow{\mathcal{D}} N(0, \mathbf{V}), \quad h\widehat{\mathbf{V}}_n = \mathbf{V}\{1 + o_P(1)\}, \quad (\text{S.8})$$

where  $\mathbf{V} = (c_2c_0 - c_1^2)^2 f(0)^2 \text{diag}(V_+, V_-)$ , and the formulas for  $V_+$  and  $V_-$  are given by  $\mathcal{V}_{+,0,1,2}^{bc}(h, b)$  and  $\mathcal{V}_{-,0,1,2}^{bc}(h, b)$  in Theorem A1(V) of [Calonico et al. \(2014\)](#), respectively. Furthermore, it also holds that  $\widehat{\mathbf{W}}_n = \mathbf{W}\{1 + o_P(1)\}$  with  $\mathbf{W} = (c_2c_0 - c_1^2)f(0)(1, 1)^T$ .

Now we proceed to prove that  $l_{\text{S,TR}}(\tau_S) \xrightarrow{\mathcal{D}} \chi_1^2$ . Let  $\widehat{\mu}_- = \arg \min_{a \in \mathcal{A}} l_{\text{S,TR}}(\tau_S, a)$ . The ratio  $l_{\text{S,TR}}(\tau_S)$  is defined as

$$l_{\text{S,TR}}(\tau_S) = 2 \sum_{i=1}^n \log \{1 + \widehat{\boldsymbol{\lambda}}^T \mathbf{Z}_i^*(\tau_S, \widehat{\mu}_-)\},$$

where  $\widehat{\boldsymbol{\lambda}} \in \mathcal{R}^2$ , and  $(\widehat{\boldsymbol{\lambda}}^\top, \widehat{\mu}_-)^\top$  is the solution to the following equations:

$$\sum_{i=1}^n \frac{\mathbf{Z}_i^*(\tau_S, a)}{1 + \boldsymbol{\lambda}^\top \mathbf{Z}_i^*(\tau_S, a)} = 0, \quad (\text{S.9})$$

$$\sum_{i=1}^n \frac{\boldsymbol{\lambda}^\top \mathbf{W}_i}{1 + \boldsymbol{\lambda}^\top \mathbf{Z}_i^*(\tau_S, a)} = 0. \quad (\text{S.10})$$

Suppose initially that  $\widehat{\mu}_- - \mu_- = O_P\{(nh)^{-1/2}\}$ . We will verify this assertion at the end of this section. Together with Equation (S.9), we obtain

$$\max_{1 \leq i \leq n} \|\mathbf{Z}_i^*(\tau_S, \widehat{\mu}_-)\|_2 = \max_{1 \leq i \leq n} \|\mathbf{Z}_i^*(\tau_S, \mu_-)\|_2 + \max_{1 \leq i \leq n} \|\mathbf{W}_i\|_2 |\widehat{\mu}_- - \mu_-| = o_P(n^{1/2}h^{-1/2}),$$

and, consequently,  $\|\widehat{\boldsymbol{\lambda}}\|_2 = O_P(n^{-1/2}h^{1/2})$ , where  $\|\cdot\|_2$  denotes the Euclidean norm. By performing a Taylor expansion for Equations (S.9) and (S.10) around  $(0, 0, \mu_-)^\top$ , we obtain

$$\begin{aligned} \widehat{\mathbf{W}}_n(\widehat{\mu}_- - \mu_-) + \widehat{\mathbf{V}}_n \widehat{\boldsymbol{\lambda}} &= \mathbf{U}_n + o_P(n^{-1/2}h^{-1/2}), \\ \widehat{\mathbf{W}}_n^\top \widehat{\boldsymbol{\lambda}} &= o_P(n^{-1/2}h^{1/2}). \end{aligned} \quad (\text{S.11})$$

Let  $\mathbf{P}_n = \mathbf{I}_2 - \widehat{\mathbf{V}}_n^{-1/2} \widehat{\mathbf{W}}_n \left( \widehat{\mathbf{W}}_n^\top \widehat{\mathbf{V}}_n^{-1} \widehat{\mathbf{W}}_n \right)^{-1} \widehat{\mathbf{W}}_n^\top \widehat{\mathbf{V}}_n^{-1/2}$ , where  $\mathbf{I}_2$  is the  $2 \times 2$  identity matrix.

Then, it follows from (S.11) that

$$\begin{aligned} \widehat{\mathbf{V}}_n^{-1/2} \mathbf{W}_n(\widehat{\mu}_- - \mu_-) &= (\mathbf{I}_2 - \mathbf{P}_n) \widehat{\mathbf{V}}_n^{-1/2} \mathbf{U}_n + o_P(n^{-1/2}) \\ \widehat{\boldsymbol{\lambda}} &= \widehat{\mathbf{V}}_n^{-1/2} \mathbf{P}_n \widehat{\mathbf{V}}_n^{-1/2} \mathbf{U}_n + o_P(n^{-1/2}h^{1/2}). \end{aligned} \quad (\text{S.12})$$

Note that  $n^{-1} \sum_{i=1}^n \mathbf{Z}_i^*(\tau_S, \widehat{\mu}_-) = \mathbf{U}_n - \widehat{\mathbf{W}}_n(\widehat{\mu}_- - \mu_-)$ ,  $h\widehat{\mathbf{V}}_n = \mathbf{V}\{1 + o_P(1)\}$ ,  $\mathbf{P}_n = \mathbf{P}\{1 + o_P(1)\}$  with  $\mathbf{P} = \mathbf{I}_2 - \mathbf{V}^{-1/2} \mathbf{W} (\mathbf{W}^\top \mathbf{V}^{-1} \mathbf{W})^{-1} \mathbf{W}^\top \mathbf{V}^{-1/2}$ . Combining these results with



(S.12),  $l_{S,TR}(\tau_S)$  can be re-expressed as

$$\begin{aligned}
l_{S,TR}(\tau_S) &= 2 \sum_{i=1}^n \log \{1 + \widehat{\boldsymbol{\lambda}}^T \mathbf{Z}_i^*(\tau_S, \widehat{\mu}_-)\} \\
&= 2 \widehat{\boldsymbol{\lambda}}^T \sum_{i=1}^n \mathbf{Z}_i^*(\tau_S, \widehat{\mu}_-) - \widehat{\boldsymbol{\lambda}}^T \sum_{i=1}^n \mathbf{Z}_i^*(\tau_S, \widehat{\mu}_-) \mathbf{Z}_i^*(\tau_S, \widehat{\mu}_-)^T \widehat{\boldsymbol{\lambda}} \{1 + o_P(1)\} \\
&= 2n \widehat{\boldsymbol{\lambda}}^T \{\mathbf{U}_n - \widehat{\mathbf{V}}_n(\widehat{\mu}_- - \mu_-)\} - n \widehat{\boldsymbol{\lambda}}^T \widehat{\mathbf{V}}_n \widehat{\boldsymbol{\lambda}} \{1 + o_P(1)\} \\
&= nh \mathbf{U}_n^T \mathbf{V}^{-1/2} \mathbf{P} \mathbf{V}^{-1/2} \mathbf{U}_n \{1 + o_P(1)\}.
\end{aligned}$$

By (S.8) and the fact that  $\mathbf{P}$  is a rank-1 projection matrix, we conclude that

$$l_{S,TR}(\tau_S) \xrightarrow{\mathcal{D}} \chi_1^2.$$

In the following, we will demonstrate that  $\widehat{\mu}_- - \mu_- = O_P\{(nh)^{-1/2}\}$ . To do so, we calculate the second derivative of  $l_{S,TR}(\tau_S, a)$  with respect to  $a$ . This derivative is strictly positive definite with probability approaching 1 within a neighborhood set  $\mathcal{A}_\delta = \{a : |a - \mu_-| \leq \delta\} \subseteq \mathcal{A}$ , where  $\delta$  is a small positive constant. Consequently,  $l_{S,TR}(\tau_S, a)$  is a convex function of  $a$  over  $\mathcal{A}_\delta$ . Note that  $l_{S,TR}(\tau_S, \mu_-) \geq l_{S,TR}(\tau_S, \widehat{\mu}_-)$ . It suffices to show that for any constant  $\varepsilon > 0$ , there exists a sufficiently large constant  $C > 0$  such that both  $l_{S,TR}(\tau_S, \mu_- - C(nh)^{-1/2})$  and  $l_{S,TR}(\tau_S, \mu_- + C(nh)^{-1/2})$  are larger than  $l_{S,TR}(\tau_S, \mu_-)$  with high probability, at least  $1 - \varepsilon$ .

Observe that  $l_{S,TR}(\tau_S, \mu_-) = 2 \log\{1 + \widehat{\boldsymbol{\lambda}}_0^T \mathbf{Z}_i^*(\tau_S, \mu_-)\}$ , where  $\widehat{\boldsymbol{\lambda}}_0$  satisfies:

$$\sum_{i=1}^n \frac{\mathbf{Z}_i(\tau_S, \mu_-)}{1 + \widehat{\boldsymbol{\lambda}}_0^T \mathbf{Z}_i^*(\tau_S, \mu_-)} = 0.$$

It can be shown that  $\widehat{\boldsymbol{\lambda}}_0 = \widehat{\mathbf{V}}_n^{-1} \mathbf{U}_n + o_P(n^{-1/2} h^{1/2})$  and  $\max_{1 \leq i \leq n} |\widehat{\boldsymbol{\lambda}}_0^T \mathbf{Z}_i^*(\tau_S, \mu_-)| = o_P(1)$ .

Hence, we have

$$l_{S,TR}(\tau_S, \mu_-) = n \mathbf{U}_n^T \widehat{\mathbf{V}}_n^{-1} \mathbf{U}_n \{1 + o_P(1)\}.$$

Analogously,  $l_{S,TR}(\tau_S, \mu_- + C(nh)^{-1/2}) = 2 \log\{1 + \widehat{\boldsymbol{\lambda}}_r^T \mathbf{Z}_i^*(\tau_S, \mu_- + C(nh)^{-1/2})\}$ , where  $\widehat{\boldsymbol{\lambda}}_r$

satisfies:

$$\sum_{i=1}^n \frac{\mathbf{Z}_i(\tau_S, \mu_- + C(nh)^{-1/2})}{1 + \widehat{\boldsymbol{\lambda}}_r^\top \mathbf{Z}_i^*(\tau_S, \mu_- + C(nh)^{-1/2})} = 0.$$

Furthermore,  $\widehat{\boldsymbol{\lambda}}_r = \widehat{\mathbf{V}}_n^{-1}\{\mathbf{U}_n - C(nh)^{-1/2}\widehat{\mathbf{W}}_n\} + o_P(n^{-1/2}h^{1/2})$  and  $\max_{1 \leq i \leq n} |\widehat{\boldsymbol{\lambda}}_r^\top \mathbf{Z}_i^*(\tau_S, \mu_- + C(nh)^{-1/2})| = o_P(1)$ . Therefore,

$$\begin{aligned} & l_{S,TR}(\tau_S, \mu_- + C(nh)^{-1/2}) \\ &= n \left\{ \mathbf{U}_n - C(nh)^{-1/2}\widehat{\mathbf{W}}_n \right\}^\top \widehat{\mathbf{V}}_n^{-1} \left\{ \mathbf{U}_n - C(nh)^{-1/2}\widehat{\mathbf{W}}_n \right\} \{1 + o_P(1)\} \\ &= n \mathbf{U}_n^\top \widehat{\mathbf{V}}_n^{-1} \mathbf{U}_n + C^2 h^{-1} \widehat{\mathbf{W}}_n^\top \widehat{\mathbf{V}}_n^{-1} \widehat{\mathbf{W}}_n - 2Cn(nh)^{-1/2} \widehat{\mathbf{W}}_n^\top \widehat{\mathbf{V}}_n^{-1} \mathbf{U}_n + o_P(1) \\ &= l_{S,TR}(\tau_S, \mu_-) + C^2 h^{-1} \widehat{\mathbf{W}}_n^\top \widehat{\mathbf{V}}_n^{-1} \widehat{\mathbf{W}}_n - 2C(n/h)^{1/2} \widehat{\mathbf{W}}_n^\top \widehat{\mathbf{V}}_n^{-1} \mathbf{U}_n + o_P(1). \end{aligned}$$

Notice that  $(n/h)^{1/2} \widehat{\mathbf{W}}_n^\top \widehat{\mathbf{V}}_n^{-1} \mathbf{U}_n = O_P(1)$ ,  $h^{-1} \widehat{\mathbf{W}}_n^\top \widehat{\mathbf{V}}_n^{-1} \widehat{\mathbf{W}}_n = \mathbf{W}^\top \mathbf{V}^{-1} \mathbf{W} \{1 + o_P(1)\}$ , and  $\mathbf{W}^\top \mathbf{V}^{-1} \mathbf{W}$  is strictly positive definite. By choosing a sufficiently large  $C > 0$ , we obtain that  $l_{S,TR}(\tau_S, \mu_- + C(nh)^{-1/2}) > l_{S,TR}(\tau_S, \mu_-)$  with probability at least  $1 - \varepsilon/2$ . Similar arguments also yield  $l_{S,TR}(\tau_S, \mu_- - C(nh)^{-1/2}) > l_{S,TR}(\tau_S, \mu_-)$  with probability at least  $1 - \varepsilon/2$ . Hence,

$$l_{S,TR}(\tau_S, \mu_- \pm C(nh)^{-1/2}) > l_{S,TR}(\tau_S, \mu_-)$$

with probability at least  $1 - \varepsilon$ . This implies that  $\hat{\mu}_- - \mu_- = O_P\{(nh)^{-1/2}\}$ . The proof for  $l_{S,TR}(\tau_S)$  is now complete.

Similar proof techniques can be applied to  $l_{S,DR}(\tau_S)$  for the sharp RDD, as well as  $l_{F,TR}(\tau_F)$  and  $l_{F,DR}(\tau_F)$  for the fuzzy RDD. See also the proof of Theorem 3.1 in [Otsu et al. \(2015\)](#). We thus complete the proofs of Theorems 3 and 4.  $\square$

## B Additional empirical results

### B.1 Nonparametric regression

In this section, we present the additional simulation results for the nonparametric regression function  $m(x)$ . Figure S1 displays the trajectories of  $m(x)$  and the evaluation points at  $x = -0.5$  for Models 1 and 2. Figure S2 plots the empirical sizes for testing  $m(x)$  at its true value under the 5% nominal level and empirical interval coverages at the 95% confidence level for all competing methods under Model 2. Table S1 reports the corresponding average empirical interval lengths and the empirical interval coverages. It is evident that our proposed robust methods (TR and DR) consistently yield the most accurate empirical sizes and coverage across all settings while offering notably narrower confidence intervals for a given  $n$  as  $h$  increases.

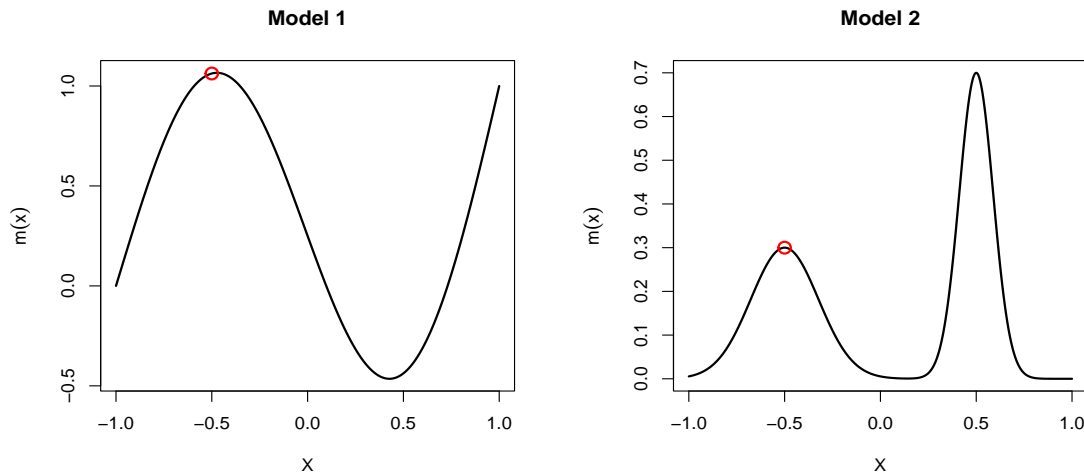


Figure S1: Regression functions for Models 1 and 2.

### B.2 Regression discontinuity design

In this section, we present the additional simulation results for the sharp RD effect  $\tau_S$ . We consider another simple low-order polynomial function given by Model 4.

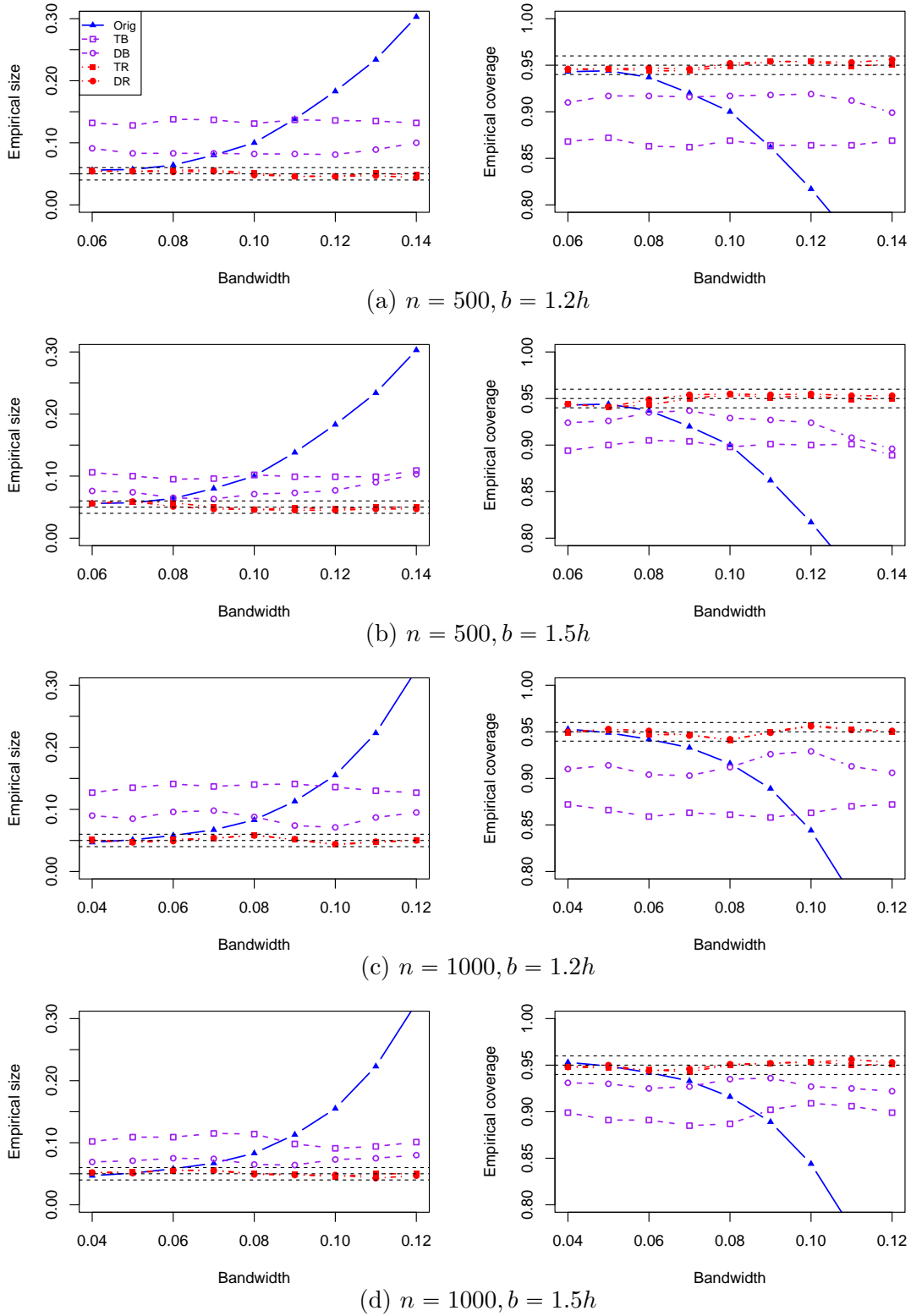


Figure S2: Plots of empirical sizes and coverages as functions of bandwidth over 1000 simulation runs at  $x = -0.5$  for Model 2.

Table S1: Average interval lengths and empirical coverages (in parentheses) of 95% confidence intervals over 1000 simulation runs at  $x = -0.5$  for Model 2. The best performances, with empirical coverages close to 95% and short interval lengths, are in bold font.

$h$	$n = 500$					$n = 1000$				
	0.06	0.08	0.10	0.12	0.14	0.04	0.06	0.08	0.10	0.12
Orig	<b>0.071</b> <b>(0.943)</b>	0.061 (0.937)	0.055 (0.900)	0.050 (0.817)	0.047 (0.697)	0.061 (0.953)	<b>0.050</b> <b>(0.942)</b>	0.043 (0.916)	0.039 (0.844)	0.035 (0.674)
Setting: $b = 1.2h$										
TB	0.071 (0.868)	0.061 (0.863)	0.055 (0.869)	0.050 (0.864)	0.046 (0.869)	0.061 (0.872)	0.050 (0.859)	0.043 (0.861)	0.039 (0.863)	0.035 (0.872)
DB	0.071 (0.910)	0.061 (0.917)	0.055 (0.917)	0.050 (0.919)	0.046 (0.899)	0.061 (0.910)	0.050 (0.904)	0.043 (0.912)	0.039 (0.929)	0.035 (0.906)
TR	0.093 (0.945)	0.080 (0.944)	0.072 (0.949)	0.066 (0.954)	<b>0.061</b> <b>(0.951)</b>	0.080 (0.949)	0.065 (0.947)	0.057 (0.941)	0.051 (0.957)	<b>0.046</b> <b>(0.950)</b>
DR	0.098 (0.946)	0.085 (0.947)	0.076 (0.952)	0.069 (0.954)	<b>0.064</b> <b>(0.956)</b>	0.085 (0.950)	0.069 (0.951)	0.060 (0.942)	0.053 (0.956)	<b>0.049</b> <b>(0.951)</b>
Setting: $b = 1.5h$										
TB	0.071 (0.894)	0.061 (0.905)	0.055 (0.898)	0.050 (0.900)	0.046 (0.889)	0.061 (0.899)	0.050 (0.891)	0.043 (0.887)	0.039 (0.909)	0.035 (0.899)
DB	0.071 (0.924)	0.061 (0.935)	0.055 (0.929)	0.050 (0.924)	0.046 (0.896)	0.061 (0.931)	0.050 (0.925)	0.043 (0.935)	0.039 (0.927)	0.035 (0.922)
TR	0.085 (0.944)	0.074 (0.943)	0.066 (0.954)	0.061 (0.953)	<b>0.056</b> <b>(0.950)</b>	0.074 (0.948)	0.060 (0.945)	0.052 (0.950)	0.047 (0.954)	<b>0.043</b> <b>(0.951)</b>
DR	0.091 (0.944)	0.079 (0.949)	0.070 (0.955)	0.065 (0.955)	<b>0.060</b> <b>(0.953)</b>	0.078 (0.948)	0.064 (0.944)	0.055 (0.951)	0.049 (0.953)	<b>0.045</b> <b>(0.953)</b>

MODEL 4.

$$m(x) = \begin{cases} x^2 & \text{if } x < 0, \\ -3x^2 + 0.5 & \text{if } x \geq 0. \end{cases}$$

See Figure S3 for the trajectories of  $m(x)$  under both Models 3 and 4. The results for Model 4 are summarized in Figure S4 and Tables S2–S3. Specifically, Figure S4 shows the empirical sizes and interval coverages based on 1000 simulations over  $h \in \{0.15, 0.18, \dots, 0.27\}$  for  $n = 500$  and  $h \in \{0.12, 0.18, \dots, 0.24\}$  for  $n = 1000$  under the settings  $b = 1.2h$  and  $b = 1.5h$ . Table S2 presents the corresponding average interval lengths and coverages. Using the MSE-optimal bandwidth selectors for  $h$  and  $b$  in Calonico et al. (2014), Table S3 provides numerical summaries under three settings with  $(h, b) = (\hat{h}_{\text{opt}}, \hat{b}_{\text{opt}})$ ,  $(\hat{h}_{\text{opt}}, 1.2\hat{h}_{\text{opt}})$  and  $(\hat{h}_{\text{opt}}, 1.5\hat{h}_{\text{opt}})$  based on 10000 replications, including the empirical sizes for  $\tau_S = 0.5$  at 5% nominal level, empirical coverages at 95% confidence level and the average interval lengths. Also presented are the average values for the selected bandwidths  $h$  and  $b$  for each setting. Similar conclusions to those in Section 5.2 can be drawn. Notably, under this simple setting, all three robust methods demonstrate strong performance in producing accurate empirical sizes and coverage, with DR continuing to slightly outperform the others when using the optimally selected bandwidth  $h$ .

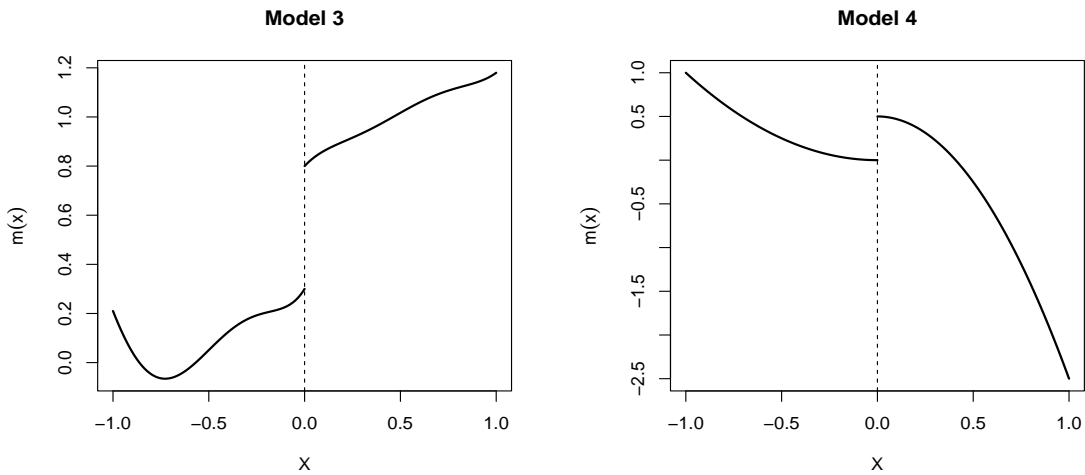


Figure S3: Regression functions for Models 3-4.

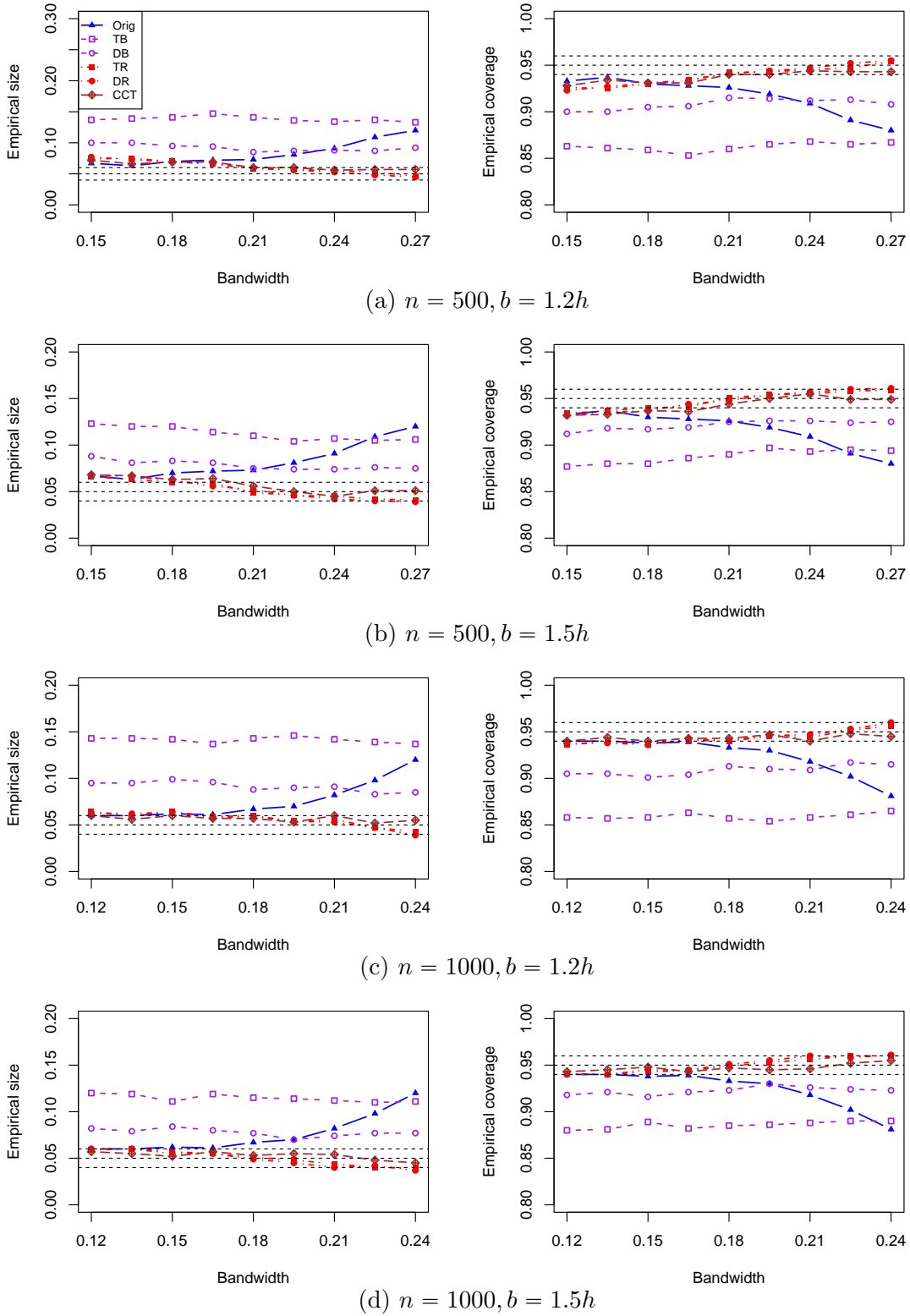


Figure S4: Plots of empirical sizes and coverages as functions of bandwidth over 1000 simulation runs for Model 4.

Table S2: Average interval lengths and empirical coverages (in parentheses) of 95% confidence intervals over 1000 simulation runs for Model 4.

$h$	$n = 500$					$n = 1000$				
	0.15	0.18	0.21	0.24	0.27	0.12	0.15	0.18	0.21	0.24
Orig	0.219 (0.933)	0.202 (0.930)	0.189 (0.926)	0.180 (0.909)	0.173 (0.880)	0.174 (0.940)	0.157 (0.938)	0.144 (0.933)	0.135 (0.918)	0.128 (0.881)
Setting: $b = 1.2h$										
TB	0.232 (0.863)	0.209 (0.859)	0.192 (0.860)	0.178 (0.868)	0.167 (0.867)	0.181 (0.858)	0.160 (0.858)	0.145 (0.857)	0.134 (0.858)	0.124 (0.865)
DB	0.216 (0.900)	0.199 (0.905)	0.186 (0.915)	0.175 (0.912)	0.166 (0.908)	0.173 (0.905)	0.156 (0.901)	0.143 (0.913)	0.133 (0.909)	0.125 (0.915)
TR	0.300 (0.926)	0.276 (0.930)	0.252 (0.942)	0.237 (0.945)	0.224 (0.954)	0.233 (0.936)	0.208 (0.936)	0.189 (0.940)	0.174 (0.944)	0.163 (0.956)
DR	0.341 (0.923)	0.291 (0.931)	0.256 (0.941)	0.239 (0.947)	0.225 (0.955)	0.238 (0.937)	0.211 (0.936)	0.190 (0.941)	0.176 (0.947)	0.164 (0.960)
CCT	0.291 (0.928)	0.266 (0.931)	0.247 (0.940)	0.232 (0.944)	0.219 (0.943)	0.232 (0.940)	0.208 (0.940)	0.190 (0.943)	0.176 (0.940)	0.165 (0.945)
Setting: $b = 1.5h$										
TB	0.225 (0.877)	0.206 (0.880)	0.190 (0.890)	0.177 (0.893)	0.167 (0.894)	0.177 (0.880)	0.159 (0.889)	0.145 (0.885)	0.133 (0.888)	0.124 (0.890)
DB	0.217 (0.912)	0.200 (0.917)	0.187 (0.925)	0.176 (0.926)	0.168 (0.925)	0.174 (0.918)	0.156 (0.916)	0.143 (0.923)	0.133 (0.926)	0.126 (0.923)
TR	0.295 (0.934)	0.258 (0.940)	0.239 (0.951)	0.225 (0.955)	0.215 (0.959)	0.218 (0.941)	0.194 (0.943)	0.177 (0.949)	0.164 (0.956)	0.154 (0.960)
DR	0.320 (0.932)	0.286 (0.937)	0.251 (0.948)	0.237 (0.957)	0.226 (0.961)	0.229 (0.940)	0.203 (0.945)	0.185 (0.951)	0.171 (0.960)	0.160 (0.961)
CCT	0.267 (0.932)	0.244 (0.937)	0.227 (0.944)	0.213 (0.955)	0.202 (0.949)	0.212 (0.943)	0.191 (0.948)	0.174 (0.947)	0.162 (0.946)	0.152 (0.955)



Table S3: Comparison of average and standard deviation (in parentheses) of bandwidths  $h$  and  $b$ , empirical sizes, empirical coverages and average interval lengths over 10000 simulation runs for Model 4.

Method	$n = 500$					$n = 1000$				
	$h$	$b$	Size	Coverage	Length	$h$	$b$	Size	Coverage	Length
Orig	0.197 (0.028)	-	0.079	0.921	0.195	0.188 (0.022)	-	0.083	0.917	0.141
					$(h, b) = (\hat{h}_{\text{opt}}, \hat{b}_{\text{opt}})$					
TB			0.093	0.907	0.196			0.083	0.917	0.140
DB			0.077	0.923	0.194			0.069	0.931	0.140
TR	0.197 (0.028)	0.350 (0.053)	0.053	0.947	0.234	0.188 (0.022)	0.362 (0.051)	0.050	0.950	0.161
DR			0.050	0.950	0.253			0.046	0.954	0.171
CCT			0.056	0.944	0.224			0.053	0.948	0.158
					$(h, b) = (\hat{h}_{\text{opt}}, 1.2\hat{h}_{\text{opt}})$					
TB			0.127	0.873	0.202			0.128	0.873	0.141
DB			0.091	0.909	0.192			0.085	0.915	0.139
TR	0.197 (0.028)	0.236 (0.033)	0.053	0.947	0.282	0.188 (0.022)	0.226 (0.026)	0.049	0.951	0.185
DR			0.052	0.948	0.294			0.048	0.952	0.187
CCT			0.053	0.947	0.258			0.050	0.950	0.185
					$(h, b) = (\hat{h}_{\text{opt}}, 1.5\hat{h}_{\text{opt}})$					
TB			0.104	0.896	0.198			0.098	0.902	0.141
DB			0.084	0.916	0.193			0.075	0.925	0.139
TR	0.197 (0.028)	0.295 (0.042)	0.051	0.949	0.251	0.188 (0.022)	0.282 (0.032)	0.047	0.953	0.173
DR			0.048	0.952	0.272			0.045	0.955	0.180
CCT			0.053	0.948	0.236			0.050	0.950	0.170

## References

- Calonico, S., Cattaneo, M. D. and Titiunik, R. (2014). Robust nonparametric confidence intervals for regression-discontinuity designs, *Econometrica* **82**: 2295–2326.
- Fan, J. and Gijbels, I. (1996). *Local polynomial modelling and its applications*, Chapman & Hall, London.
- Otsu, T., Xu, K.-L. and Matsushita, Y. (2015). Empirical likelihood for regression discontinuity design, *Journal of Econometrics* **186**: 94–112.
- Owen, A. B. (2001). *Empirical likelihood*, Chapman and Hall/CRC.